The biofluorescence-bleaching method for distinguishing caries lesion from discolored pit and fissure

Hyung-Suk Lee

The Graduate School

Yonsei University

Department of Applied Life Science

The biofluorescence-bleaching method for distinguishing caries lesion from discolored pit and fissure

Directed by Professor Baek-Il Kim

A Doctoral Dissertation
Submitted to the Department of Applied Life Science
And the Graduate School of Yonsei University
in partial fulfillment of the requirements
for the degree of Doctor of Philosophy in Dental Science

Hyung-Suk Lee

June 2024

This certifies that the Doctoral Dissertation of

Hyung-Suk Lee is approved.

Thesis Supervisor: Baek-Il Kim

Thesis Committee: Ho-Keun Kwon

Thesis Committee: Ki-Ho Chung

Thesis Committee: Su-Jung Shin

Thesis Committee: Hoi-In Jung

The Graduate School

Yonsei University

June 2024

Acknowledgements

연구자의 길을 향한 학위의 도전은 2012년에 시작한 뒤, 지난 시간 꿈을 향해 열심히 달려왔고, 2024년 드디어 마무리하게 되었습니다. 석사를 마무리하고 이어서 군복무, 다시 박사 과정, 그 누구보다 길었던 학위 과정 동안 아낌없는 격려와 많은 도움을 주신 모든 분께 감사의 글을 올립니다.

연구의 방향을 제시해주고 어려웠던 연구 주제를 쉽게 풀 수 있도록 지도해주시고 깊은 고찰과 학문의 가치를 끌어내 주신 김백일 지도교수님께 깊은 존경과 감사를 드립니다. 부족하지만 교수님께서 항상 믿고 지켜봐 주신 덕분에 차곡차곡 연구를 마무리할 수 있었습니다. 놓치기 쉽고 생각하지도 못했던 의견을 제시해주시고 통계적 의미와 해석에 많은 도움을 주신 정회인 교수님 감사드립니다. 항상 볼 때마다 응원해주시고 의국 생활 동안 문화, 예술을 누릴 수 있도록 해 주신 권호근 교수님께 깊이 존경의 마음을 표현합니다. 임상적 자문과 의견을 아낌없이 조언해주신 신수정 교수님, 완성도 높은 논문을 위해 귀중한 조언해주신 정기호 교수님께도 마음 깊이 감사드립니다. 결과 정리와 해석을 하는데 세심한 조언을 해 주신 이은송 교수님 감사합니다.

오랜 시간 동안 의국에 있으면서 많은 선후배님들과 함께 하였습니다. 거의 매일 함께 동고동락을 하면서 서로 격려를 해주고 많은 힘이 되어준 예방치과학 교실의 의국원들에게 고마운 마음을 전하고 싶습니다. 이제는 든든하고 함께 학위 심사 준비하면서 꼼꼼하게 챙겨준 최준혁 선생님, 열정과 에너지 넘치고 옆 자리에서 끊임

없이 응원해준 박솔, 묵묵히 응원해주고 교실의 중심 의국장 이채현 선생님, 교실의 엔돌핀 조합 김아름, 조연지 선생님, 앞으로 더욱 기대되는 막내 최아현, 포은 선생님, 과제 담당할 때 많이 도와줬던 김채연 선생님, 힘들었던 의국 생활의 든든한 지원군들이 되어주어서 감사했습니다. 감사의 마음을 전하다보니 지난 의국 생활 동안 함께 했던 선생님들도 생각이 나네요. 김희은, 한선영, 김영석, 강시묵, 구혜민, 정은하, 이주영, 김상겸, 박석우, 김효정, 김은수, 조무열 선생님, 같은 길을 걸어가며 함께 응원해주신 선후배 선생님들을 만난 것은 제 인생의 가장 큰 행복이었습니다. 외부에서 격려해주시고, 학교 밖에서의 정보를 공유해주시는 서동구, 조남억, 맹유진, 황혜림, 이현중, 전미경, 남상미, 김예슬, 황지현, 정명진, 이선영, 강건웅 선생님 항상 큰 힘이 되어주셔서 정말 감사합니다. 큐레이 연구를 지속할 수 있도록 지원해주시고 응원해주신 윤홍철 원장님 감사합니다. Dr. Elbert, professor Inaba and Matsukubo, thank you for big help and friendly support!

많은 분들의 배려와 응원 덕분에 좋은 결실을 맺을 수 있었습니다. 모든 분들께 감사한 마음을 표현하기에는 지면이 한정되어 있어 송구스럽습니다. 앞으로 학위 과정 중에 받았던 많은 사랑과 격려를 돌아보며 잊지 않고 더욱 열심히 하겠습니다.

끝으로 오랜 공부를 하는 동안 저를 믿어주시고 변함없이 헌신적으로 지원해주신 부모님 사랑하고 정말 감사합니다. 이제는 어엿하게 성장하여 유종의 미를 거둘 수 있게 도와준 동생도 감사합니다.

2024년 7월 이형석 올림

CONTENTS

List of Figures

List of Tables

Abstract

The biofluorescence-bleaching method for distinguishing caries lesion from discolored pit and fissure

Hyung-Suk Lee

Department of Applied Life Science

The Graduate School, Yonsei University

(Directed by professor Baek-Il Kim)

The occlusal surface of teeth has narrow and deep pits and fissures, making it easy for staining substances to attach and allowing for the accumulation of external deposits such as dental plaque. Due to the complex anatomical structure of the occlusal surface, removing deposits from pits and fissures is difficult, leading to susceptibility to occlusal caries. During this process, if bacteria penetrate the demineralized porous structure concurrently

with staining substances, it progresses to brown or black opaque cariogenic discoloration. Pit and fissure discoloration is among the factors impacting the diagnosis of occlusal caries and plays a pivotal role in confirming its presence. However, distinguishing between discoloration caused by the caries process and stains originating from organic substances such as food chromogens is challenging for dentists in clinical settings. Furthermore, using discoloration as a diagnostic criterion for occlusal caries still remains controversial.

The biofluorescence (BF) technology utilized in dental field visualizes and quantifies the BF emitted from teeth when exposed to the short wavelength of blue visible light, evaluating the pathological state of the oral cavity. Changes in mineral contents and structure within dental tissues manifest as differences in green BF intensity, while pathological conditions related to oral bacteria metabolism can be identified by red BF intensity. There have been efforts to differentiate cariogenic discolorations on occlusal tooth surfaces using BF. However, assessing BF from discolored occlusal surfaces has limitations due to the masking effect of discoloration, which absorbs and scatters light. Therefore, this study aims to verify the BF color changes of pits and fissures before and after bleaching, and to suggest BF-bleaching as a method to detect occlusal caries after removing organic stains from discolored occlusal surfaces.

The present study was conducted in two main experiments. The first experiment aimed to distinguish cariogenic discoloration by comparing the BF color changes after applying BF-bleaching to a simulation model mimicking cariogenic discoloration. In the second experiment, BF-bleaching was applied to the discolored pits and fissures of extracted teeth,

and the changes in BF color parameters were examined to confirm their ability to distinguish cariogenic discoloration.

In the first study, artificial early caries lesions mimicking cariogenic discoloration were created using bovine incisors to reproduce the BF observed in cariogenic discoloration. These lesions were classified into three categories: non-stained lesions (NS) without any staining intervention, organic-stained (OS), and cariogenic-stained (CS) lesions. Dental bleaching was performed to remove stains, and the BF changes of discolored lesions were evaluated both fluorometrically and hyperspectrally. As the stains were removed through bleaching, the BF of the lesions tended to brighten. However, within the CS group, the hue angle ($h°$) of BF persisted within the red color range (345°–15°), and the second emission peak within the red range (620–780 nm) of the BF spectrum distinctly observable. In contrast, the $h°$ of BF in the OS group exhibited a significant shift from orange (15°–45°) to yellow (45°–75°) after bleaching, but there was no second emission peak in the red range of the BF spectrum.

In the second study, bleaching was applied to extracted teeth with discolored pits and fissures, and the BF color changes were evaluated on individual pit and fissure analysis units. Histology results were utilized to differentiate between non-cariogenic discoloration, referred to as sound area (Sound), and cariogenic discoloration (CD). Additionally, CD was further classified into two categories based on the presence of red BF observed in BF images on occlusal surfaces before bleaching: cariogenic discoloration accompanied by red BF (RF) and cariogenic discoloration without observed red BF (Non-RF). Before bleaching,

the red BF intensity (ΔR) differed significantly among the Sound, Non-RF, and RF groups. After 5 minutes of bleaching, the ΔR of the Non-RF and RF groups became similar. The BF $h°$ of the RF and Sound groups increased over time after bleaching, maintaining the red and orange ranges, respectively. In contrast, the $h°$ of the Non-RF group decreased after bleaching, with the color range shifting from orange to red. The ability of the BF parameters to distinguish between Sound and Non-RF groups, where no red BF was observed before bleaching, was confirmed through ROC analysis. The ROC analysis revealed improvements in sensitivity, specificity, and the area under the ROC curve (AUROC) for both ΔR and $h°$ parameters after bleaching. Particularly, the sensitivity of the ΔR increased significantly from 0.79 to 0.90 five minutes after bleaching, and the AUROC of $h°$ also showed a sharp improvement from 0.69 to 0.93. After bleaching, all BF parameters exhibited high validity of 0.83 or higher in distinguishing cariogenic discoloration.

In conclusion, the application of BF-bleaching to discolored pit and fissure areas led to a BF color change, confirming the removal of organic stains due to bleaching. In contrast, the red BF of cariogenic discoloration persisted even after bleaching. Particularly, the ability to distinguish cariogenic discoloration using ΔR and $h°$ parameters notably improved five minutes after bleaching, effectively demonstrating high validity post-bleaching. Therefore, BF-bleaching is expected to be a promising method for objectively distinguishing cariogenic discoloration and monitoring caries lesions in clinical settings.

Key words: Discolored caries lesion, Discolored pit and fissure, Cariogenic discoloration, Organic stain, Biofluorescence, Dental bleaching, Biofluorescence-bleaching.

The biofluorescence-bleaching method for distinguishing caries lesion from discolored pit and fissure

Hyung-Suk Lee

Department of Applied Life Science

The Graduate School, Yonsei University

(Directed by professor Baek-Il Kim)

I. Introduction

In recent decades, with evolving trends in dental caries and an enhanced comprehension of the caries process, there has been a noticeable increase in the prevalence of non-cavitated lesions relative to the overall experience of dental caries (Carvalho, 2014). In particular, occlusal surfaces, such as pits and fissures, have complex and discontinuous

anatomical structures, making them more susceptible to microbial attack and attachment compared to smooth surfaces (Carvalho, 2014; Carvalho et al., 2016). When bacteria residing in dental biofilm adhering to the occlusal surfaces become metabolically active, they produce acids, thereby initiating demineralization, which leads to the loss of minerals from dental hard tissues and increases the porosity of enamel surfaces (Kidd and Fejerskov, 2004). This porous structure exhibits white opacity due to differences in refractive index to light compared to sound tooth structure (Hariri et al., 2013). During this demineralization process, staining substances from food, beverages, or medications that easily adhere to the occlusal surfaces can become involved. When bacteria penetrate the porous structure concurrently with the staining substances, it can lead to the progression of brown or black opaque cariogenic discoloration (Lee et al., 2018; Watts and Addy, 2001).

Discoloration frequently presents in pits and fissures, constituting a significant factor in the diagnostic assessment of occlusal caries (Kordic et al., 2003; Steiner et al., 1998). A previous study utilized pit and fissure discoloration for occlusal caries assessment via visual inspection, revealing a specificity of 0.17 and a comparatively higher sensitivity of 0.68 (Lussi, 1993). Histological analysis of transverse sections of discolored pits and fissures confirmed the presence of extensive caries lesions beneath them, imperceptible on the tooth surface (Christensen et al., 2001). Meanwhile, there have also been negative opinions regarding the use of discoloration of the occlusal surface as a diagnostic criterion for dental caries. Previous research has highlighted the potential for overestimation when employing occlusal surface discoloration as a diagnostic indicator, resulting in

approximately 70% unnecessary restorative interventions (Kordic et al., 2003). Notably, despite the discolored pits and fissures actually being sound, 55% were inaccurately assessed as caries lesions (Lussi, 1993). Therefore, it is crucial to distinguish cariogenic discoloration from discolored pits and fissures, as the presence of discoloration in pits and fissures does not necessarily indicate caries lesions. Currently, there is insufficient evidence to support the use of discoloration as a diagnostic criterion for occlusal caries, rendering the issue a matter of ongoing debate (Abu-Hanna and Mjör, 2008). Consequently, there arises a necessity for the development of adjunctive diagnostic methods capable of preventing misdiagnosis of discolored occlusal caries while providing clear evidence to distinguish cariogenic discoloration from discolored pits and fissures (Kapor et al., 2021).

In recent years, in the field of dentistry, adjunct diagnostic methods utilizing the characteristics of biofluorescence (BF) have been employed to complement the limitations of traditional methods for diagnosing dental caries and to provide objective information (Pretty, 2006). BF refers to light with longer wavelengths emitted after absorbing high-energy, short-wavelength light by living organisms (Hakanson et al., 2022; Mazel, 2017). In particular, blue visible light with a wavelength of 405 nm is typically utilized in dentistry. Upon exposure to this light, sound teeth exhibit blue-green (460–560 nm) BF, whereas dental plaque and caries lesions, involving metabolites of oral bacteria, exhibit red (600–700 nm) BF (Walsh and Shakibaie, 2007). By utilizing these properties, changes in the hard tissue structure or mineral content in dental tissues can be identified by differences in green BF intensity, while pathological conditions caused by oral bacteria can be quantified by the

intensity of red BF, derived from the metabolite porphyrin (Lee et al., 2023; Oh et al., 2022; Park et al., 2019). Numerous previous studies have utilized these properties of BF to detect various oral conditions, including changes in hard tissues such as tooth cracks and wear, as well as oral bacteria-related dental caries and pathological dental biofilms (Han et al., 2016; Jun et al., 2019; Jung et al., 2018; Kim et al., 2020).

Efforts have been made to distinguish cariogenic discoloration by utilizing the BF properties exhibited in discolored pits and fissures. A previous study evaluated discolored pits and fissures by calculating the green BF intensity, which is useful for predicting the depth of caries lesions. This study confirmed that this green BF parameter effectively distinguishes cariogenic discoloration with high validity (Lee et al., 2018). However, discoloration has characteristics that absorb or scatter light, which can result in lower measurements of green BF intensity and subsequently reduce diagnostic performance (Amaechi and Higham, 2002). Therefore, numerous previous studies have recommended excluding teeth with discoloration in pits and fissures when evaluating occlusal caries using optical methods (Côrtes et al., 2003; Kordic et al., 2003). Meanwhile, a previous study has reported that the red BF parameter can compensate for the shortcomings of the green BF intensity parameter, and it has been confirmed that the red BF intensity parameter can also effectively distinguish cariogenic discoloration with high validity (Lee et al., 2018). However, red BF is not observed in all cariogenic discolorations, and in deep pits and fissures, it is difficult to completely remove external debris or dental plaque, which can reduce the accuracy of the BF parameters (Jung et al., 2018; Oh et al., 2022). Considering

these facts, it is necessary to prioritize the removal of superficial staining substances from pits and fissures before evaluation to enhance the ability of all BF parameters to detect cariogenic discoloration.

Dental bleaching is one of the non-invasive method for chemically removing discoloration from pits and fissures. This method utilizes redox reactions between bleaching molecules and chromophore molecules. In dentistry, hydrogen peroxide is used for effective bleaching treatments. The reactive oxygen species in hydrogen peroxide penetrate the enamel and dentin matrix and break down complex chromophore molecules that cause dark discoloration into simpler molecules. Molecules broken down into simpler structures reflect less light, resulting in brighter teeth (Kwon and Wertz, 2015). Most dental bleaching agents are formulated as gels, which provide good accessibility to anatomically complex pits and fissures. They also offer the advantages of short application times and cost efficiency (Al-Angari and Hara, 2016; Watts and Addy, 2001). A previous study has mentioned that using dental bleaching to alter the color of discolored pits and fissures can enhance the ability to detect caries lesions in these areas (Falconer et al., 2008). Considering that cariogenic discoloration occurs due to chromophores of staining substances penetrating the porous structure caused by demineralization, dental bleaching is considered a useful method to improve caries detection by removing organic stains that confound caries diagnosis.

To the best of our knowledge, there have been no studies conducted to evaluate occlusal caries following the removal of stains from pits and fissures. Furthermore, there

have been no reported studies assessing BF changes resulting from the application of bleaching to discolored caries lesions. Therefore, this study employed the BF-bleaching method as a key technique to evaluate BF changes after removing stain through dental bleaching. To achieve this, we aimed to evaluate BF changes before and after bleaching using a simulation model that mimics the BF characteristics observed in cariogenically discolored teeth in a laboratory setting, as well as in extracted teeth with naturally discolored pits and fissures.

The aim of this study was to investigate the BF color changes of discolored pits and fissures before and after dental bleaching and to propose the BF-bleaching method as a technique for detecting occlusal caries after removing organic stains from cariogenically discolored teeth. The specific objectives of this study are as follows:

i. To evaluate the feasibility of distinguishing between organic stains and cariogenic discoloration by applying the BF-bleaching method to a simulation model that mimics cariogenic discoloration and comparing the BF color changes of both types of discoloration.
ii. To investigate the changes in BF color parameters following the application of the BF-bleaching method to discolored pits and fissures in extracted teeth.
iii. To evaluate the validity of the BF-bleaching method in enhancing the ability to distinguish cariogenic discoloration from actual discoloration in pits and fissures through comparative analysis.

II. Materials and Methods

2.1. Study design

This study was conducted through two main experiments. The BF-bleaching method was used to evaluate the BF color change after performing dental bleaching to remove organic stains from cariogenically discolored teeth, utilizing both bovine incisors and extracted human teeth.

In the first study, bovine incisors were used to simulate the BF changes observed in cariogenically discolored teeth in a laboratory setting. Porphyrin was used to reproduce the red BF, a representative metabolic product of oral bacteria, and it was stained along with organic staining in artificial caries lesions. Denta bleaching was then performed on the stained enamel, and the BF changes were evaluated using fluorescence and hyperspectral imaging techniques.

In the second study, extracted teeth were used with the subjects' consent, and the study was approved by the Institutional Review Board of Yonsei University Dental Hospital (IRB No. 2-2020-0083). First, teeth with discolored pits and fissures on the occlusal surface were visually and radiographically evaluated to assess the severity of caries. Afterward, BF color changes following bleaching of the occlusal surface were evaluated at the individual pits and fissures analysis unit. Finally, the evaluated areas were histologically sectioned to assess the severity of caries, and based on these results, the ability to distinguish cariogenic discoloration in BF color parameters before and after bleaching was confirmed.

2.2. BF-bleaching application to an *in vitro* simulation model mimicking cariogenic discoloration (Study 1)

2.2.1. Specimen preparation

Thirty sound bovine incisors without cracks, wear, white spots, fluorosis, or enamel hypoplasia were selected for the study. To obtain areas of uniform enamel thickness on the labial surface of bovine incisors, specific flat areas measuring 8 × 6 × 3 mm were designated, and enamel specimens were obtained by sectioning with a low-speed handpiece equipped with a diamond disc (NTI-KAHLA GmbH, Kahla, Germany). The specimens were then positioned within acrylic molds sized 20 × 12 × 7 mm, with a hole diameter of 9 mm, and embedded using self-curing resin (Ortho-Jet, Lang Dental Manufacturing, Wheeling, Illinois, USA). To achieve a flat surface on all specimens, sequential polishing was carried out using water-cooled equipment (RB 209 Minipol, R&B Inc., Daejeon, Republic of Korea) with 600, 1000, 1200, and 1500 grit SiC sandpaper (R&B Inc., Daejeon, Republic of Korea).

2.2.2. Group allocation

This study initially induced artificial early caries lesions in bovine enamel to simulate cariogenic discoloration. In the lesion group, cariogenic-stained lesions (CS) were designated, with organic-stained lesions (OS) and early caries lesions without staining (NS) serving as the positive and negative control groups, respectively, for comparison with CS (Figure 1). For fair group allocation, the surface hardness of polished specimens was measured using a microhardness tester (MMT-X, Matsuzawa, Akita, Japan). The Vickers indenter was applied for 10 seconds with a load of 200 g at three points on the central and lateral surfaces of the enamel to measure the Vickers microhardness number (VHN), after which the mean value was calculated. The mean VHN (standard deviation) of all specimens was 319.63 (9.60). The VHN value of each specimen was sorted in ascending order, and ten specimens were allocated to each of the three groups: NS, OC, and CS (Kim et al., 2009).

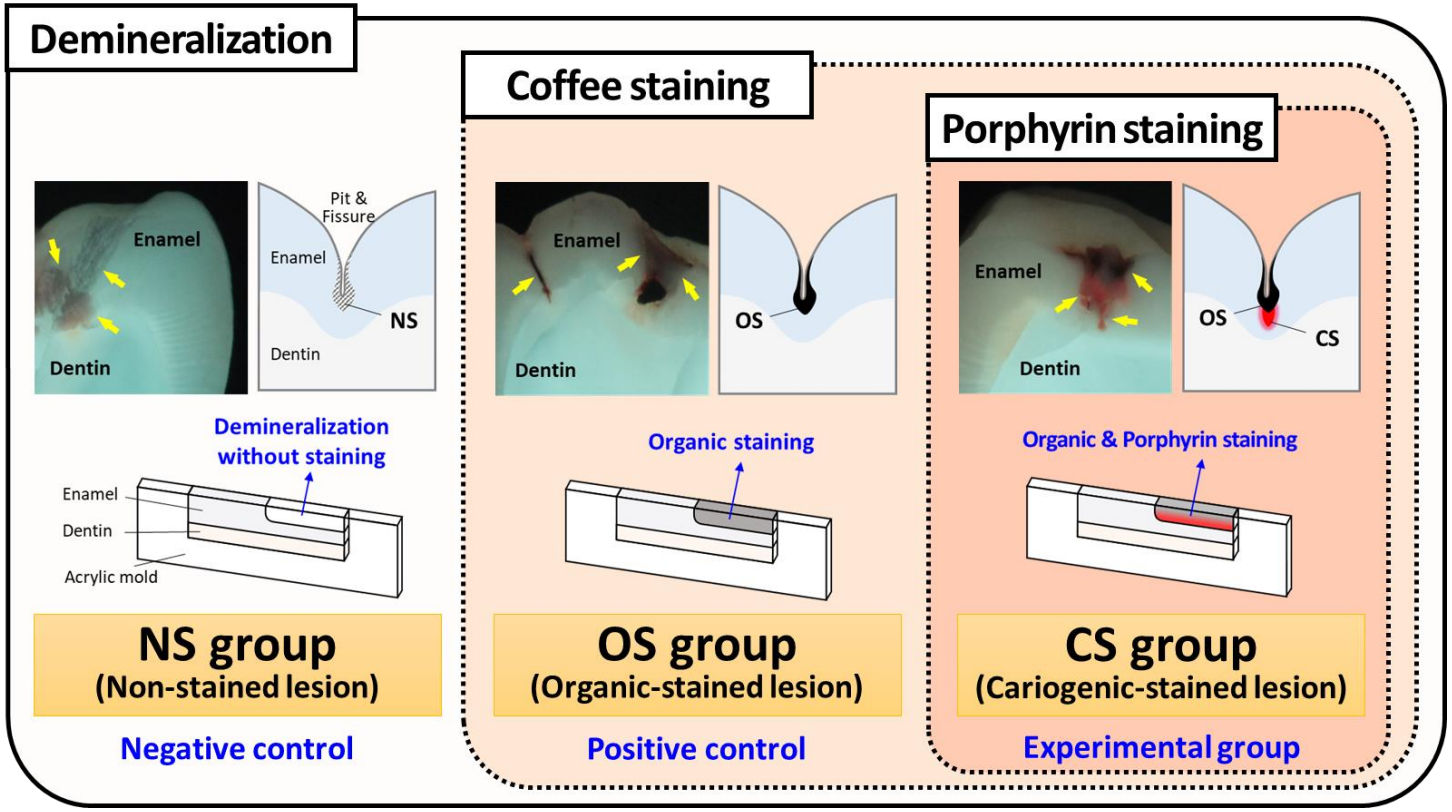

Figure 1. The groups of simulated cariogenic discoloration model.

2.2.3. Artificial caries lesion creation

Prior to the formation of artificial caries lesions, half of the surface of each polished specimen was protected by attaching acid-resistant acrylic to preserve the sound enamel as a reference area. The demineralizing solution was formulated by saturating 50% hydroxyapatite (calcium phosphate tribasic, Sigma, St. Louis, MO, USA) in 0.1 M lactic acid and 2% Carbopol polymer (Carbopol EDT 2050, Noveon Inc., Wickliffe, OH, USA), with the final pH adjusted to 4.8 (White, 1987). The dried specimens were hydrated by immersion in distilled water for 30 minutes, followed by immersion of each specimen in 40 ml of demineralizing solution and maintenance at 37℃ for 5 days to create subsurface lesions. After demineralization, the residual demineralizing solution on the specimen surface was rinsed off with distilled water.

2.2.4. Staining

In this study, different types of staining solutions were penetrated for each group into the surface porous structure of artificial caries lesions formed after demineralization to form OS and CS lesions (Figure 2). For the OS group, commercially available coffee powders (Beanist® Original Americano, EDIYA Coffee, Seoul, Republic of Korea) were used, and 10 g/L of powder was dissolved in distilled water according to the manufacturer's recommendations. The CS group prepared a PPIX solution by dissolving 0.4 mM (PPIX, Aldrich, Milwaukee, USA), a metabolite of representative cariogenic bacteria, in 1:1 ratio distilled water and dimethyl sulfoxide solution to simulate actual caries lesion expressing red BF (Mendes et al., 2006). Each specimen was immersed in the staining solution and stirred for 24 hours to induce staining. In the CS group, the red BF observed in the lower part of real caries lesions and the staining caused by organic substances in the upper part were reproduced. To achieve this, the specimens were first immersed in a PPIX solution for 24 hours and then dried. Subsequently, they were immersed in organic staining solution for an additional 24 hours to induce staining. The lesions were then remineralized to reflect the state of real pit and fissure caries of the occlusal surface, resulting in the formation of inactive arrested caries lesions.

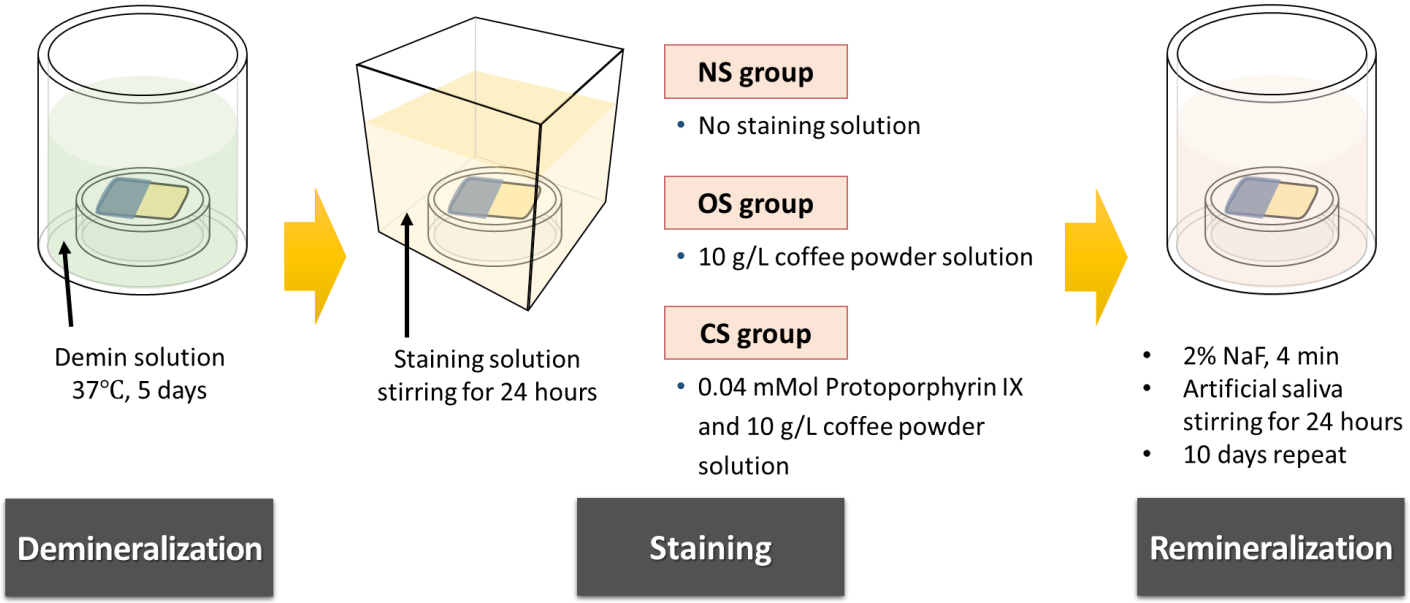

Figure 2. Demineralization, staining, and remineralization for creating discolored caries lesion.

2.2.5. Remineralization

For the remineralization of the lesions, the specimens were immersed in a 2% sodium fluoride (NaF) solution for 4 minutes (Figure 2). After immersion, the specimens were taken off, and any remaining NaF solution on the surface was rinsed off with distilled water. Subsequently, each specimen was immersed in artificial saliva (0.22% mucin, 30 mM KCl, 10 mM KH_2PO_4, 13 mM NaCl, 3 mM $CaCl_2$, final pH 6.8; refilled daily) for an additional day (24 hours) (Park et al., 2022). The remineralization of initial caries lesions was conducted for 10 days, and after completion of remineralization, the acid-resistant acrylic tape covering each specimen was removed. The specimens were places in impermeable containers capable of blocking external light until analysis, and stored refrigerated at 4℃.

2.3. BF-bleaching application to extracted teeth having discolored pit and fissure (Study 2)

2.3.1. Teeth sample selection

The study was conducted after obtaining ethical approval from the Institutional Review Board for Clinical Research at Yonsei University Dental Hospital (IRB No. 2-2020-0083). Permanent human teeth that had been freshly extracted for orthodontic, periodontal, or prosthetic purposes were collected from participants aged 20 and above who voluntarily enrolled and provided informed written consent. Among the collected teeth, 122 permanent premolars and molars suspected of caries lesion due to discoloration on the pits and fissures of occlusal surfaces were selected (Figure 3). Teeth having distinct cavity, advanced proximal caries, or extensive demineralized lesions on smooth surfaces were excluded among the selected teeth. Moreover, teeth exhibiting excessive calculus or dental plaque accumulation, or where extrinsic deposits could not be removed due to deep pits and fissures, were likewise excluded, resulting in a total of 93 teeth finally utilized for this study. Upon extraction, the teeth were immediately immersed in distilled water, followed by removal of residual tissues, calculus, and plaque adhering to the tooth surfaces using manual toothbrushes and scalers. Subsequently, the teeth were rinsed and then stored frozen at −20℃ in a light-blocking black container to prevent BF degradation of caries lesion until evaluation (Hope et al., 2011).

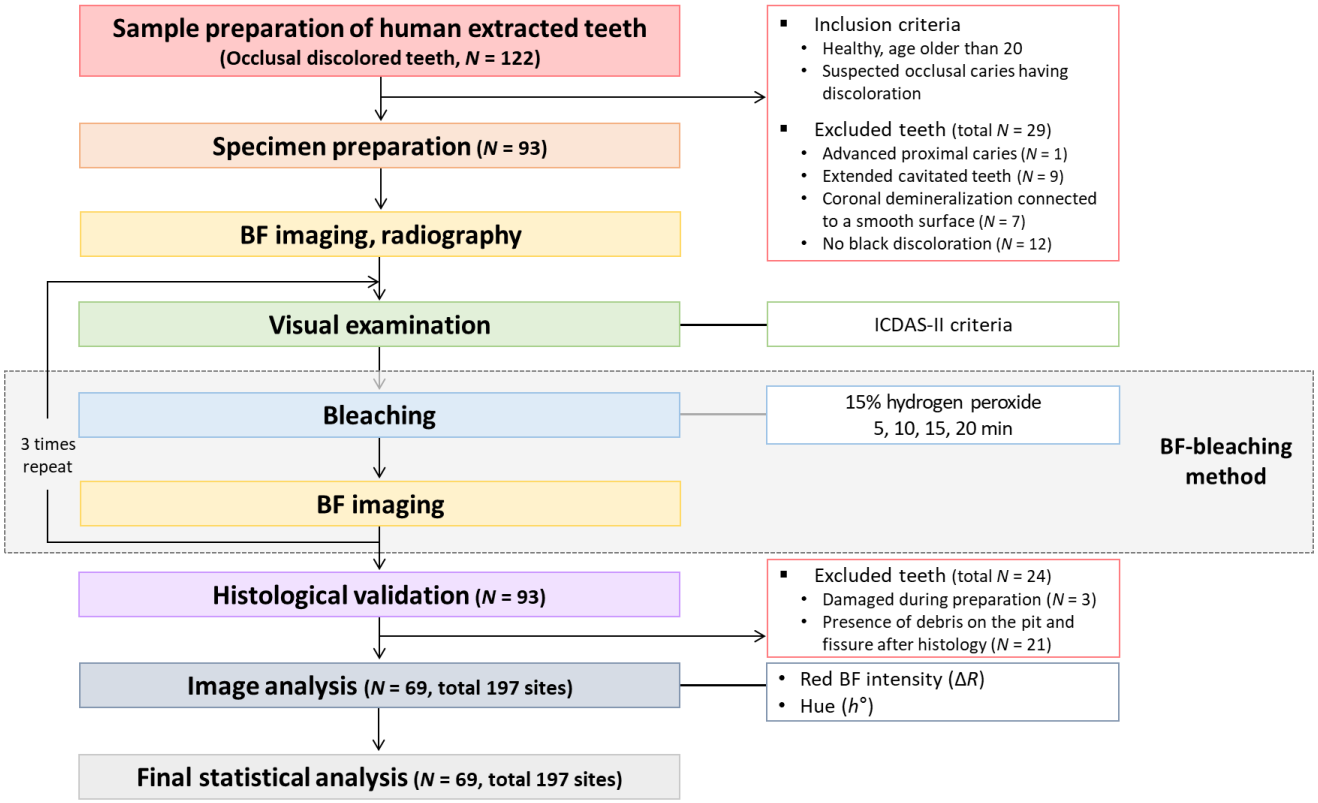

Figure 3. Flow chart of study 2.

2.3.2. Specimen preparation

To ensure uniform height of the tooth specimens, root areas exceeding 1.5 cm from the highest cusp point of the occlusal surface were sectioned using a low-speed handpiece equipped with a diamond bur (NTI-KAHLA GmbH, Kahla, Germany). Subsequently, each tooth specimen was fixed by vertically inserting the root area into a 9 mm diameter hole within a 20 × 12 × 7 mm acrylic mold and securing it with self-curing resin (Ortho-Jet, Lang Dental Manufacturing, Wheeling, Illinois, USA). The tooth specimens were then stored at 4℃ in a state of 100% humidity to prevent dehydration throughout all evaluation processes.

2.3.3. Visual examination

The presence and severity of occlusal caries were assessed using compressed air and a WHO probe, according to the criteria of the International Caries Detection and Assessment System (ICDAS) II (Dikmen, 2015). This study evaluated the pits and fissures of the occlusal surfaces corresponding to ICDAS scores 0 to 4, representing stages prior to distinct cavity formation. In accordance with the guidelines outlined in the ICDAS classification criteria manual, the assessment of occlusal caries included considerations of discoloration-related aspects in addition to changes in translucency on the surface (Table 1).

Table 1. Visual examination criteria for caries lesion severity

ICDAS score	Description (pits and fissures)
0	**Sound tooth surface:** no change in enamel translucency after 5 seconds air drying
1	**First visual change in enamel:** When seen wet there is no evidence of any change in color but after 5 seconds air drying a carious opacity or discoloration is visible that is not consistent with the clinical appearance of sound enamel and is limited to the confines of the pit and fissure area
2	**Distinct visual change in enamel:** When wet there is a carious opacity and/or brown carious discoloration which is wider than fissure (the lesion is still visible when dry)
3	**Localized enamel breakdown due to caries with no visible dentine or underlying shadow:** When wet there is a carious opacity and/or brown carious discoloration which is wider than fissure. Once dried for approximately 5 seconds there is carious loss of tooth structure at the entrance to, or within, the pit of fissure/fossa but dentin is not visible in the walls or base of the discontinuity.
4	**Underlying dark shadow from dentine with or without enamel breakdown:** This lesion appears as a shadow of discolored dentin visible through an apparently intact enamel surface which may or may not show signs of localized breakdown. The darkened area may appear as grey, blue or brown in color and is seen more easily when the tooth is wet.

ICDAS, International Caries Detection and Assessment System

2.3.4. Radiography

Radiographs of the tooth specimens were taken using dental X-ray equipment (Kodak 2200 Intraoral X-ray System, Eastman Kodak Co., Rochester, NY, USA). The radiographs were obtained at a distance of 3 cm from the tooth specimens and 5 cm from the sensor, with the X-ray equipment holder cone positioned, employing 60 kV voltage and 7 mA current, with an exposure time of 0.096 seconds. Subsequently, the radiographs were displayed on a 27-inch monitor using radiographic viewer software (PiViewSTAR, Infinitt, Seoul, KR), and evaluated under identical lighting conditions. The brightness and contrase of the radiographs were adjusted considering the clinical situation. Evaluation was conducted according to the criteria in Table 2 (Pitts, 1984), and representative images for each criterion were presented in Figure 4.

Table 2. Radiographical criteria for caries lesion severity

Radiographical score	Description
0	No radiolucency
1	Radiolucency restricted to the outer half of the enamel
2	Radiolucency involved inner half of enamel, up to (including) dentinoenamel junction
3	Radiolucency confined to outer half of dentine
4	Radiolucency involved inner half of dentine with/without apparent pulpal involvement

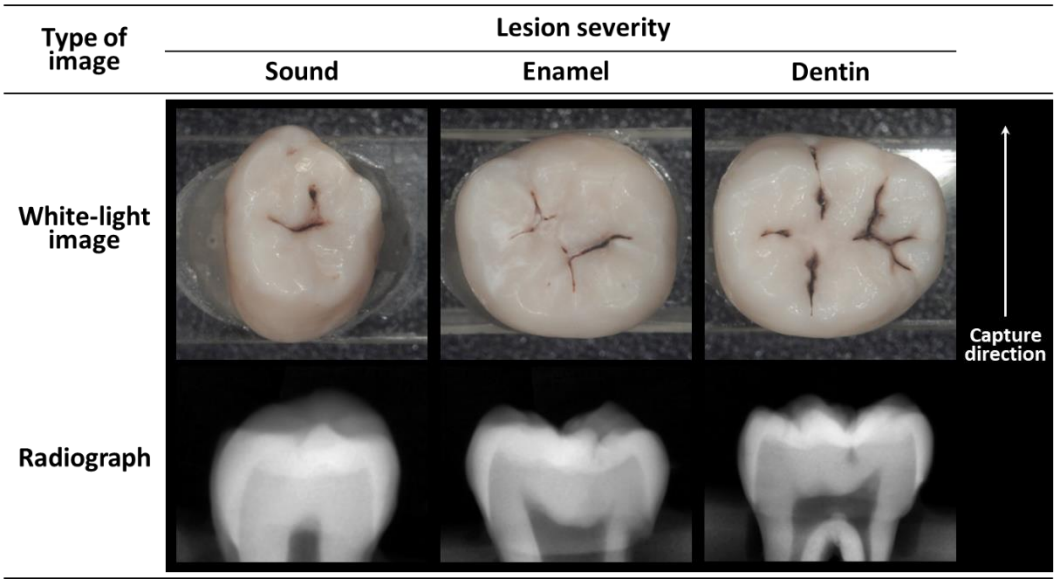

Figure 4. Representative radiographs according to the caries severity. Sound, no radiolucency; Enamel, radiolucency in the enamel; Dentin, radiolucency involving the dentin.

2.4. Dental bleaching

This study employed dental bleaching agents to bleach the occlusal surfaces to evaluate changes in BF of discolored lesions before and after bleaching. The experiment was conducted by taking photographs with imaging equipment before and after bleaching procedure. For bleaching the occlusal surfaces of all specimens, a dental bleaching agent containing 15% hydrogen peroxide (BeauTis 15 whitening, Osstempharma, Seoul, Republic of Korea) was used (Figure 5). The bleaching procedure was conducted at 5-minute intervals for a total duration of 20 minutes.

Figure 5. Dental bleaching agents and its application in the study.

2.4.1. Study 1

Before bleaching, the tooth specimens were hydrated. The bleaching agent was then applied to the enamel surface of each specimen in a uniform thickness of 0.5 to 1.0 mm, maintaining 100% relative humidity at 37℃. After bleaching, the remaining bleaching agent on the enamel surface was rinsed off with distilled water, and the specimens were dried for BF imaging. The bleaching procedure was conducted at 5-minute intervals for a total duration of 20 minutes.

2.4.2. Study 2

Before bleaching, the tooth specimens were hydrated, and compressed air was used to remove moisture from the pits and fissures to ensure proper application of the bleaching agent. The bleaching agent was then applied to fill the pits and fissures of each specimen, maintaining 100% relative humidity at 37℃. After bleaching, the bleaching agent was rinsed off with distilled water, and any residual agent in the pits and fissures was removed using compressed air and water. The bleaching procedure was conducted at 5-minute intervals for a total duration of 20 minutes.

2.5. Biofluorescence imaging

2.5.1. Quantitative light-induced fluorescence imaging (Study 1 and 2)

To obtain BF images of the tooth specimens and evaluate the BF of the discolored areas, the Quantitative Light-induced Fluorescence-Digital 2+ Biluminator (QLF-D, Inspektor Research Systems BV, Amsterdam, The Netherlands) was utilized. The QLF-D device is optimized for BF imaging, equipped with 12 blue LEDs emitting light at a wavelength of 405 nm and 4 white LEDs (6500K) mounted on a DSLR camera. First, the QLF-D was positioned perpendicularly to the occlusal surface of the specimens, maintaining a consistent distance from the imaging area. Ambient light that could affect BF image acquisition was then blocked. Using the proprietary BF imaging software (C3 v1.27, Inspektor Research Systems BV), BF images were captured under the following conditions: a shutter speed of 1/30 s, an aperture value of 8.0, and an ISO speed of 1600. BF images were taken before and immediately after bleaching, at 5-minute intervals for a total duration of 20 minutes.

2.5.2. Hyperspectral biofluorescence imaging (Study 1)

A hyperspectral camera (Pika L, Resonon Inc., Bozeman, MT, USA) was utilized to obtain hyperspectral BF spectra of tooth specimens (Figure 6). To acquire the hyperspectral data of BF emitted from tooth specimens upon irradiation with a 405 nm light source, the illumination system of the apparatus was furnished with 12 blue LEDs (405 nm) and 4 white LEDs (6500K). A Ef-S 60mm f/2.9 macro lens (Canon Inc., Tokyo, Japan) equipped with a >460 nm cutoff filter was attached to the hyperspectral camera. For hyperspectral BF spectrum imaging at each time point before and after bleaching of discolored lesions, the dedicated software SpectrononPro (v.3.4.0, Resonon Inc., Bozeman, MT, USA) was utilized. Each specimen was placed on an imaging stage, and the light source was directed perpendicular to the surface of specimen. The images were captured under conditions where external light was blocked. The hyperspectral BF spectrum was captured while scanning the tooth specimen in a line-scanning mode with a 2 nm interval, covering the final range between 420 nm and 820 nm. The BF spectrum imaging was performed for a total of 20 minutes, at 5-minute intervals, both before and immediately after bleaching.

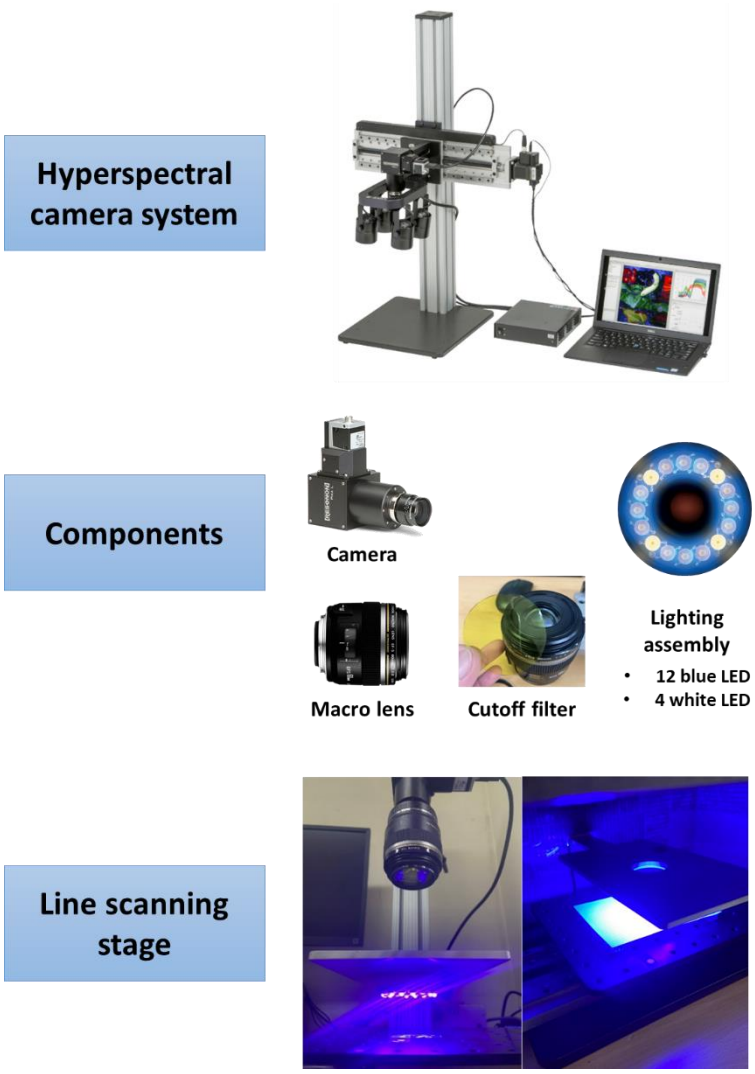

Figure 6. Hyperspectral camera system.

2.6. Biofluorescence color analysis

In the BF images, quantitative parameters such as red BF intensity (ΔR) and BF hue angle ($h°$) were utilized to evaluate the BF color of the discolored lesions. For the calculation of these BF color parameters, BF images were analyzed using proprietary QLF-D image software (QA2 v1.27, Inspektor Research Systems BV, Amsterdam, The Netherlands), in conjunction with image analysis software (Image J version 1.51o, National Institutes of Health, Bethesda, MD, USA).

2.6.1. Analysis patch designation

To calculate the ΔR values explaining the difference in BF color intensity of the discolored area (evaluation area) compared with the sound enamel (reference area), both the evaluation area and the reference area were included in the analysis patch. Conversely, for the calculation of the $h°$ value, which describes the hue of the evaluation area itself, the analysis patch was limited to the discolored area (Figure 7).

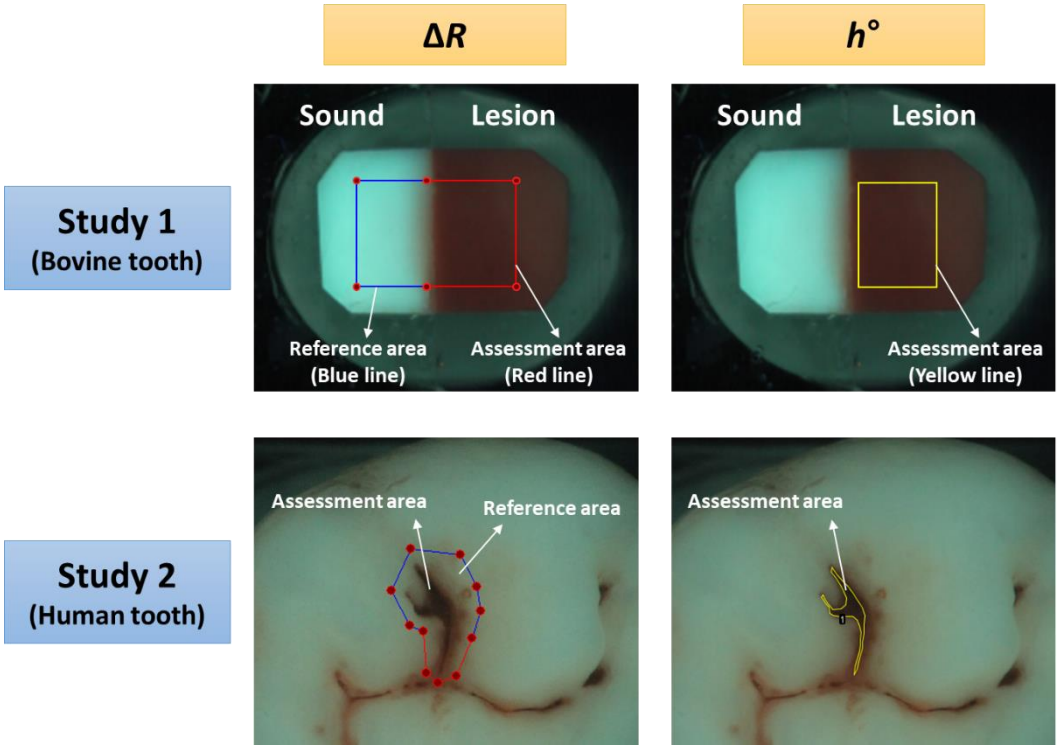

Figure 7. Analysis patches for this study.

2.6.1.1. Study 1

For the calculation of the ΔR value, a rectangular analysis patch measuring 6 × 4 mm was drawn on the central area of the enamel surface in the BF image and subsequently saved. At this time, the sound enamel area was designated as the reference region using active contour points. The discolored lesion area (evaluation area) was specified as a disabled contour point to prevent referencing and then saved (Figure 7). In the determination of the $h°$ value, an analysis patch within the discolored area was drawn using the polygon selection feature in the BF image, and subsequently specified and saved.

2.6.1.2. Study 2

The designation of analysis patches for BF color analysis was conducted by setting all pits and fissures of the occlusal surface as analysis units. For the calculation of the ΔR value, analysis patches were drawn along the areas up to 2 mm away from the pits and fissures of the occlusal surface suspected of caries lesions due to discoloration in the BF image, and then saved. At this time, areas similar to the BF color of surrounding sound enamel were designated as active contour points (reference areas), while areas difficult to reference due to discoloration were designated as disable contour points (evaluation areas), and then saved (Figure 7). For the calculation of the $h°$ value, an analysis patch ($Patch_{Discolored}$) was drawn along the boundary of the area that appeared different in color from the sound tooth, based on the pits and fissures in the white-light image, and then used.

2.6.2. Increase in red biofluorescence intensity

When comparing the BF of the lesion area illuminated by blue visible light to that of sound enamel, the degree of bacterial metabolism can be quantified by the increase in red BF intensity, expressed as ΔR (%). The analysis patches previously saved in the QA2 software were imported into the BF image, and the ΔR value of the tooth specimens was calculated. The ΔR value was automatically calculated by the analysis software based on the RGB color system using the R, G, and B values obtained from the BF image, according to the following formula:

$$\Delta R = [(R/G)_D - (R/G)_S] / (R/G)_S$$

where ΔR represents the relative red BF intensity of the lesion area compared to that of sound enamel, R is the intensity of red, G is the intensity of green, D is the discolored area, and S is the sound enamel.

2.6.3. Biofluorescence hue angle

The BF hue of the discolored area was determined by the hue angle in the HSV system and calculated using Image J software (Figure 8). First, the BF image was converted into an 8-bit grayscale image in the single color system (L^*, a^*, b^* channels) of the CIE Lab color system using the 'convert to' function of the analysis software. The previously saved $Patch_{Discolored}$ was imported into the converted grayscale image, and the L^*, a^*, and b^* values of the discolored area were calculated. In this color system, the a^* variable of the green-red coordinates (where a negative a^* indicates green and a positive a^* indicates red) and the b^* variable of the blue-yellow coordinates (where a negative b^* indicates blue and a positive b^* indicates yellow) were utilized. The L^* variable, representing brightness (achromatic coordinate), was excluded from the analysis (Lee, 2014). In the BF image, the BF hue information excluding brightness was calculated as a hue angle ($h°$) on a 360-degree circular scale using the following formula, and the BF color of the lesion before and after bleaching was assessed based on the color region corresponding to the $h°$ value:

$$h° = \arctan(b^* / a^*).$$

Here, $h°$ represents the BF hue angle of lesion area, a^* denotes the green-red coordinate, and b^* signifies the blue-yellow coordinate.

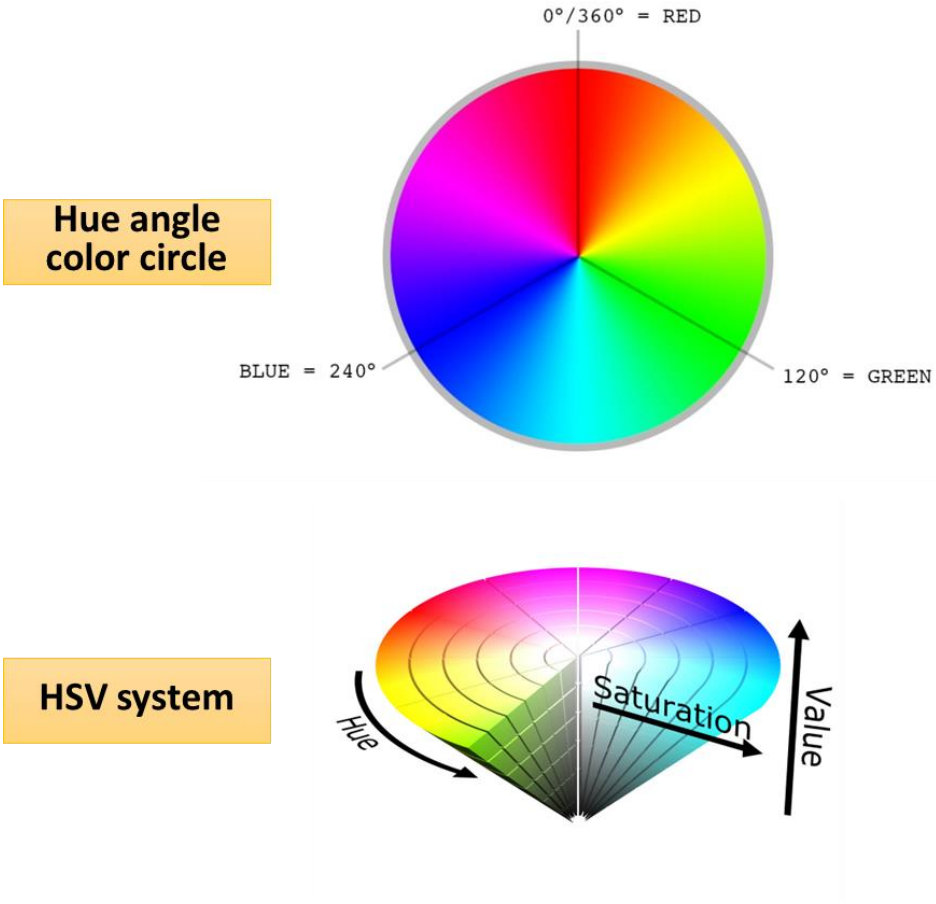

Figure 8. Hue angle of the HSV system.

2.6.4. Hyperspectral biofluorescence spectrum (Study 1)

Hyperspectral BF spectra data were obtained using SpectrononPro software. First, the same regions interest used in previous analyses for patches of discolored areas (evaluation areas) were selected in the hyperspectral BF images. Then, the output information of BF emitted under 405 nm light source illumination was obtained. This data was subsequently extracted into Excel format files (Microsoft 365, Microsoft corporation, Redmond, WA, USA), and the BF spectrum was plotted. To examine the hyperspectral BF color changes in discolored areas of each group before and after bleaching, all spectra were normalized and compared. At this point, the BF spectra obtained from the specimens of each discolored group were normalized by setting the intensity value of the first emission peak in the 480–520 nm wavelength range to 100%. The spectrum of sound enamel area was used as reference spectrum to compare with the BF spectra of discolored lesions. The wavelengths of all peak points in the spectra of each group before and after bleaching were identified, and the shifts in the spectra due to bleaching were observed.

2.7. Histology

2.7.1. Study 1

After completing all evaluations, a line parallel to the long axis of the tooth specimen was designated as the region of interest. A low-speed diamond microtome (TechCut 4™, Allied High Tech Products, Inc., CA, USA) was used to obtain a 1 mm thick section for histological evaluation, including the region of interest. Subsequently, the section was polished under continuous water supply with 800 grit SiC sandpaper until the thickness of the section reached approximately 150 μm. The polished section was photographed at 400× magnification using polarized-light microscope (PLM; CX31-P, Olympus, Tokyo, Japan). The depth of the lesion in the microscope images was measured using Image J software, and the presence of a remineralized surface layer was verified.

2.7.2. Study 2

After completing all evaluations, all pits and fissures present on the occlusal surface were designated as individual regions of interest and sectioned. A low-speed diamond microtome (TechCut 4^{TM}) was used to obtain histological sections perpendicular to the occlusal surface. Subsequently, the section was polished under continuous water supply with 800 grit SiC sandpaper until the thickness of the section reached approximately 150 μm. A QLF-D equipped with a high-magnification macro lens (Canon EF 100mm f/2.8L Macro IS USM, Canon Inc., Tokyo, Japan) was positioned perpendicularly to the polished surface of the sections, and then BF images were captured (Figure 9). The obtained BF images were used to assess the presence and severity of caries lesions in the evaluation area by scoring the maximum lesion area according to the classification criteria in Table 3 (Figure 10).

Figure 9. QLF-D equipped with a macro lens.

Table 3. Histological criteria for caries lesion severity

Histological score	Description
S	No enamel demineralization or narrow surface zone of opacity (edge phenomenon)
E1	Enamel demineralization limited to the outer 50% of the enamel layer
E2	Demineralization involving the inner 50% of enamel up to the dentinoenamel junction
D	Demineralization involving the outer 50% of the dentine

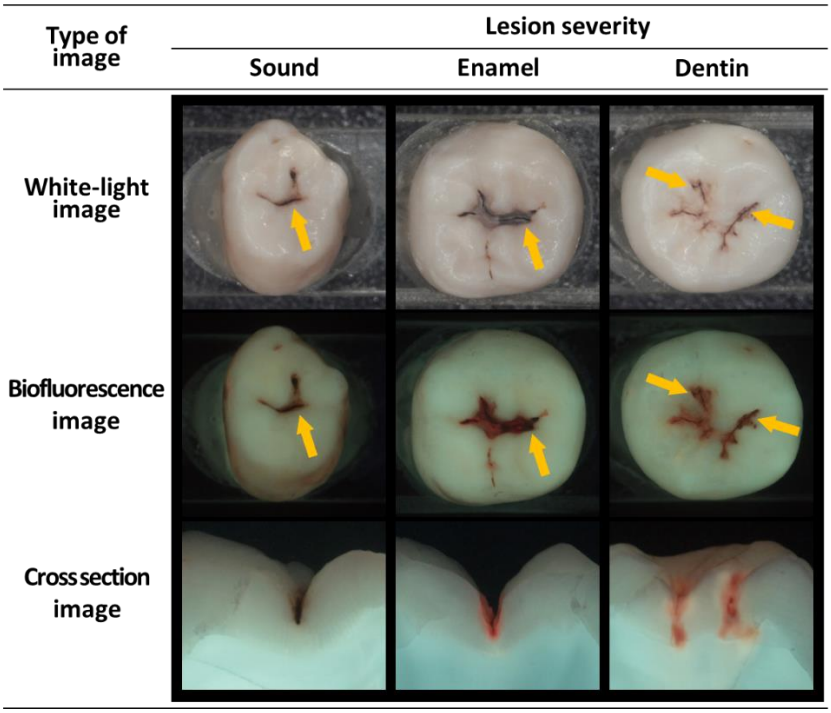

Figure 10. Representative images of occlusal surfaces and cross sections obtained from QLF-D. Yellow arrows indicate the sectioned sites.

2.8. Statistical analysis

The differences in red BF intensity (ΔR) and hue angle ($h°$) for each discolored lesion group were tested for normality using the Kolmogorov-Smirnov test. If the data were normally distributed, one-way ANOVA was used; if not, the Kruskal-Wallis test was performed. All statistical analyses were conducted at a significance level of 0.05 using SPSS 26.0 (IBM Corp., Armonk, NY, USA).

2.8.1. Study 1

Statistical tests were performed on the differences in red BF intensity (ΔR) and hue angle ($h°$) of discolored lesions compared to sound enamel. The differences in parameters between discolored lesion groups at each time point were analyzed using one-way ANOVA. Changes in BF color of lesions over bleaching time within the same lesion group were compared using one-way ANOVA. The lesion depths of each lesion group were compared using one-way ANOVA. For parameters showing significant differences, Bonferroni *post-hoc* analysis was performed.

2.8.2. Study 2

The distribution of caries severity according to ICDAS-II, radiographic examination, and histological examination results was determined through frequency analysis.

2.8.2.1. Operational definition of discolored pit and fissure

To distinguish discolored pits and fissures, the operational definitions from a previous study were used (Lee et al., 2018). Based on the histological examination results, discolored teeth were dichotomized into the sound (noncariogenic discoloration) group for sound teeth and the cariogenic discoloration (CD) group for carious teeth. Additionally, the CD group before bleaching was further subdivided into the Non-RF group and the RF group based on the presence or absence of red BF observed in the occlusal pits and fissures in the BF images (Figure 11).

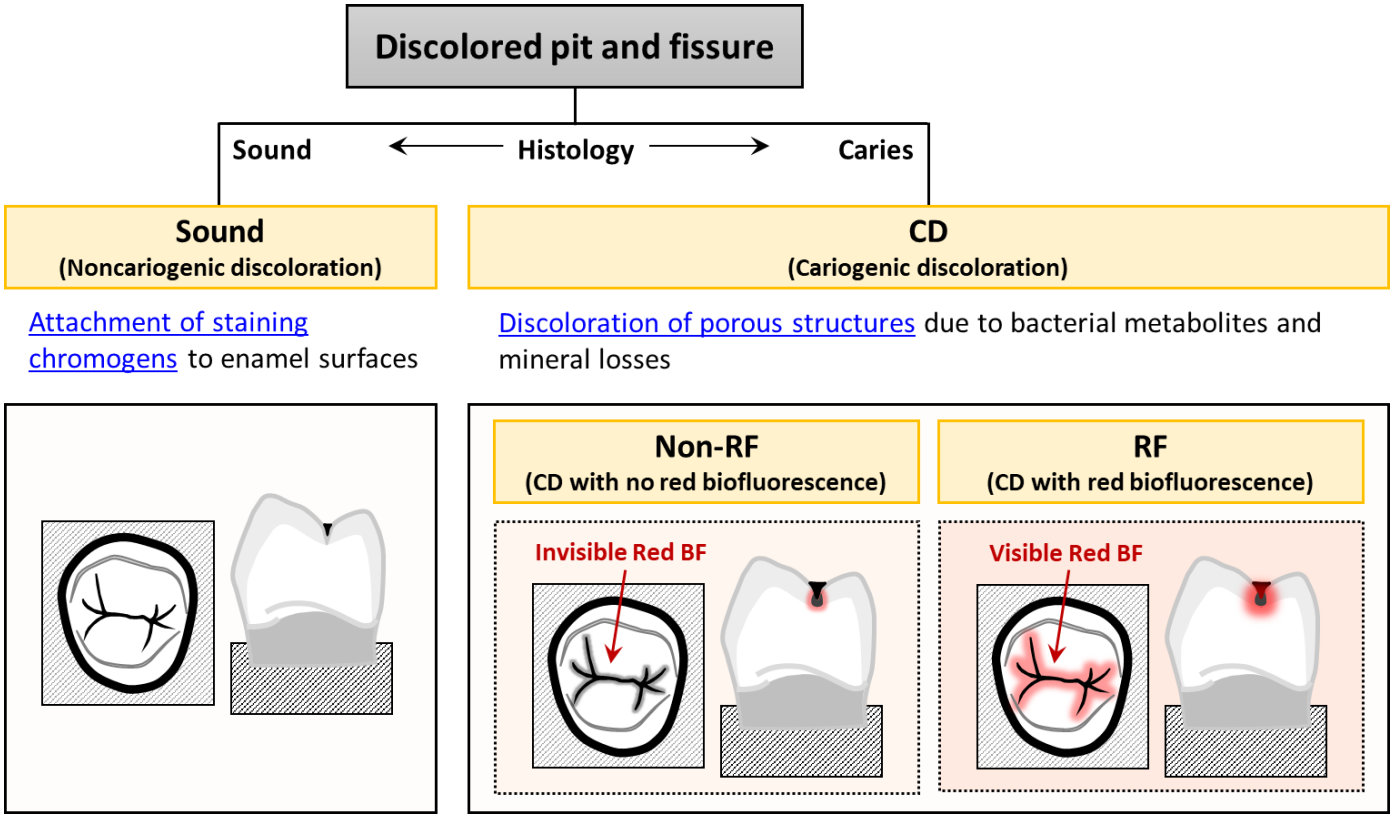

Figure 11. The groups of tooth discoloration.

2.8.2.2. Changes in color and biofluorescence parameters

Statistical analyses were performed on the differences in red BF intensity (ΔR) and the hue angle ($h°$) of the discolored lesions compared to sound enamel. Differences in parameters between discolored lesion groups at each bleaching time point were analyzed using the Kruskal-Wallis test and the Mann-Whitney test. The changes in BF color of discolored lesions over bleaching time within the same lesion group were also compared using the Kruskal-Wallis test and the Mann-Whitney test. For parameters showing significant differences, Bonferroni *post-hoc* analysis was performed.

2.8.2.3. Diagnostic performance of biofluorescence parameters

To confirm the ability of BF color parameters to distinguish cariogenic discoloration before and after bleaching, sensitivity and specificity were calculated based on Sound and Non-RF groups, and a Receiver operating characteristic (ROC) analysis was performed and compared. The ROC analysis was conducted using MedCalc (version 22.023, MedCalc Software Ltd., Ostend, Belgium).

III. Results

3.1. Changes in biofluorescence properties of the cariogenic discoloration model after dental bleaching (study 1)

Histological evaluation of the discolored lesion specimens showed that the lesion depths (in μm) for the NS, OC, and CS groups were similar, with values of 35.56 ± 2.77, 36.56 ± 3.15, and 34.22 ± 3.22, respectively.

3.1.1. Color changes in discolored lesion area in the white-light image

Observation of the white-light images revealed that the NS group, which was not stained, appeared white, whereas the CS and OS groups, which involved staining, appeared dark brown. Furthermore, the discolored lesions in the CS and OS groups were observed to be similar in color, making it difficult to distinguish between the two groups (Figure 12).

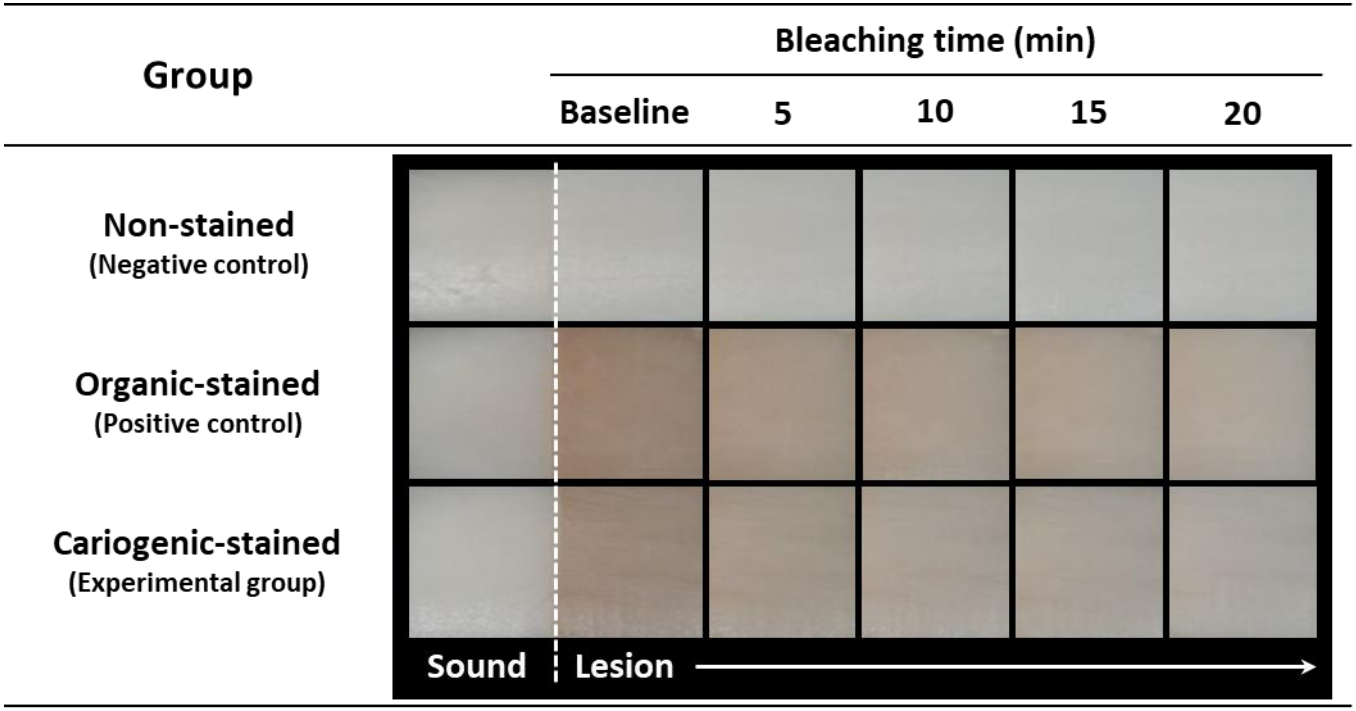

Figure 12. Representative white-light images of a simulation model mimicking cariogenic discoloration in relation to the duration of dental bleaching.

The sound and lesion parts of each specimen are on the left and right, respectively.

3.1.2. Increase in red biofluorescence intensity of discolored lesion area compared to the sound enamel

Observation of the BF images revealed that both the sound enamel and the lesion areas in the NS group exhibited green BF. In contrast, the BF colors in the CS and OS groups, which included staining, were different: the CS group showed dark red BF, while the OS group displayed dark brown BF. This color difference allowed for clear distinction between the two groups (Figure 13). Both discolored lesion groups exhibited a tendency for BF to lighten as bleaching progressed. The calculation of the red BF intensity of the discolored lesions compared to sound enamel in the BF images showed that the ΔR values were significantly different among the three groups at all time points before and after bleaching ($p<0.001$, Table 4). The ΔR value of the NS group was 0% at all time points, indicating that no red BF was observed. At baseline, the ΔR value of the CS group was approximately 2.74 times higher than that of the OS group ($p<0.001$). After 20 minutes of bleaching, the ΔR value of the CS group remained approximately 1.73 times higher than that of the OS group ($p<0.001$). After 10 and 20 minutes of bleaching, the ΔR value of the CS group decreased by 41% and 61%, respectively, compared to baseline. In the OS group, the ΔR value decreased by 20% and 43%, respectively ($p<0.001$, Figure 14).

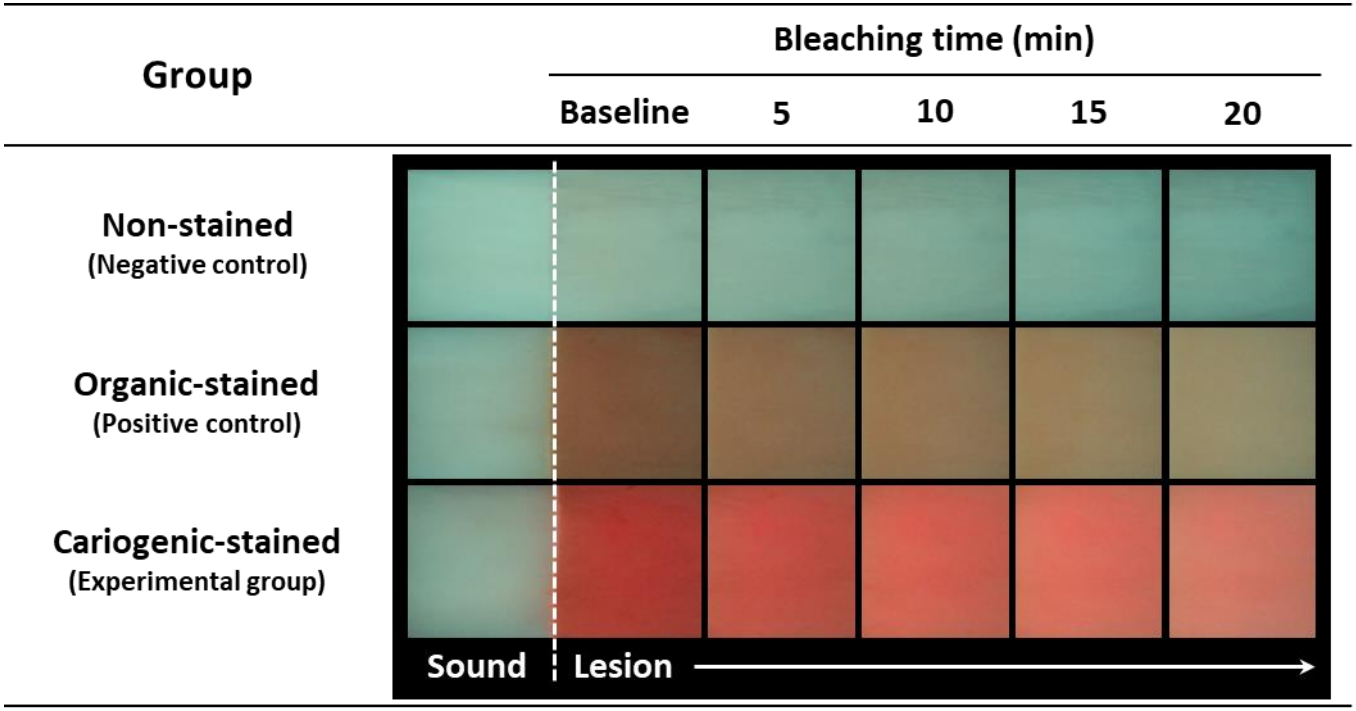

Figure 13. Representative biofluorescence images of a simulation model mimicking cariogenic discoloration in relation to the duration of dental bleaching.

The sound and lesion parts of each specimen are on the left and right, respectively.

Table 4. Differences in red biofluorescence intensity (Δ*R*, %) between sound enamel and caries lesion parts for each group, with respect to bleaching time (n = 10 in each group).

Δ*R* (%)	Bleaching time (min)				
Groups	Baseline	5	10	15	20
Non-stained (Negative control)	0.00 ± 0.00 $^{A, a}$	0.00 ± 0.00 $^{A, a}$	0.00 ± 0.00 $^{A, a}$	0.00 ± 0.00 $^{A, a}$	0.00 ± 0.00 $^{A, a}$
Organic-stained (Positive control)	75.59 ± 7.66 $^{B, a}$	70.38 ± 8.02 $^{B, b}$	60.35 ± 8.01 $^{B, c}$	49.23 ± 7.41 $^{B, d}$	43.45 ± 9.42 $^{B, e}$
Cariogenic-stained (Experimental group)	207.41 ± 21.94 $^{C, a}$	161.97 ± 22.99 $^{C, b}$	122.35 ± 20.66 $^{C, c}$	98.73 ± 15.60 $^{C, d}$	75.12 ± 13.11 $^{C, e}$

All values are means ± standard deviations.
Different capital letters (A–C) within the same column indicate significant differences between groups by one-way analysis of variance with Bonferroni *post-hoc* test ($p<0.05$).
Different lowercase letters (a–e) within the same row indicate significant differences between bleaching time points by one-was analysis of variance with Bonferroni *post-hoc* test ($p<0.05$).

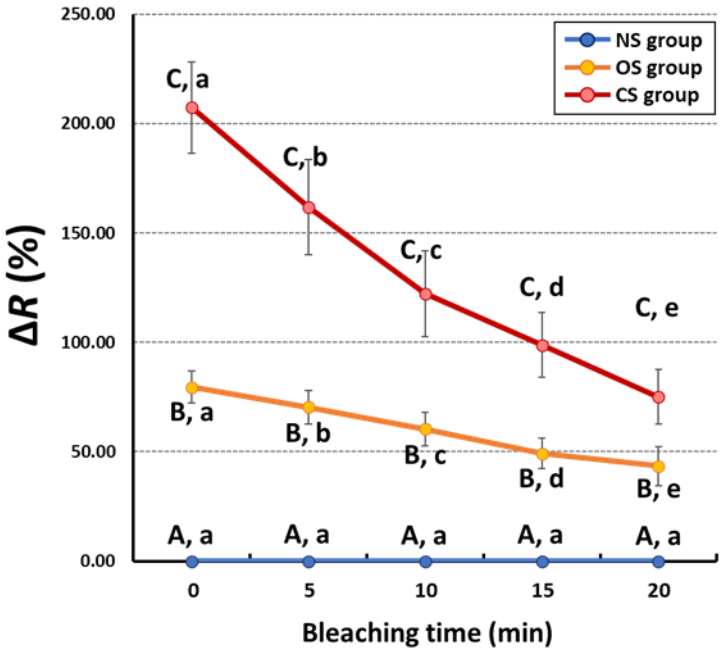

Figure 14. Changes in the differences in red biofluorescence intensity (Δ*R*, %) between sound enamel and caries lesion parts with respect to bleaching time for each group (n = 10 in each group).

NS, non-stained; OS, organic-stained; CS, cariogenic-stained lesion group.
Different capital letters (A–C) indicate significant differences between groups by one-way analysis of variance with Bonferroni *post-hoc* test ($p<0.05$).
Different lowercase letters (a–e) indicate significant differences between bleaching time points by one-way analysis of variance with the Bonferroni *post-hoc* test ($p<0.05$).

3.1.3. Biofluorescence hue angle of discolored lesion area

By analyzing the hue angle ($h°$) values to determine the hue regions of each discolored lesion group, it was found that the BF hue emitted by the CS group was located in the red region. In contrast, the OS and NS groups exhibited BF in the orange and green regions, respectively. The $h°$ value of the CS group showed no significant difference between baseline (4.60°) and after 10 minutes of bleaching (7.70°) (Table 5). After 20 minutes of bleaching, the $h°$ value of the CS group significantly increased by approximately 8.1° compared to baseline ($p<0.001$), but it remained within the same red region (345–15°) (Figure 15). In contrast, the OS group was located in the orange region (15–45°) at baseline. After 20 minutes of bleaching, the $h°$ value increased by approximately 21.9°, shifting the hue region to the yellow range (45–75°) ($p<0.001$). The NS group remained in the green region (135–165°) at all bleaching time points. The $h°$ value of the NS group showed no difference between baseline (149.80°) and after 10 minutes of bleaching (153.60°), but it significantly increased after 20 minutes of bleaching (163.50°) ($p<0.001$).

Table 5. Differences in biofluorescence hue angle (*h*°) of caries lesion parts for each group, with respect to bleaching time (n = 10 in each group).

h° (degree)	Bleaching time (min)				
Groups	Baseline	5	10	15	20
Non-stained (Negative control)	149.80 ± 7.32 $^{A, a}$	151.80 ± 6.73 $^{A, a}$	153.60 ± 5.40 $^{A, a}$	159.70 ± 5.08 $^{A, b}$	163.50 ± 3.75 $^{A, b}$
Organic-stained (Positive control)	24.10 ± 0.88 $^{B, a}$	28.90 ± 1.91 $^{B, b}$	30.10 ± 2.33 $^{B, b}$	35.30 ± 3.16 $^{B, c}$	46.00 ± 4.52 $^{B, d}$
Cariogenic-stained (Experimental group)	4.60 ± 1.51 $^{C, a}$	6.20 ± 1.99 $^{C, a}$	7.70 ± 2.21 $^{C, a}$	9.50 ± 3.03 $^{C, a, b}$	12.70 ± 3.53 $^{C, b}$

All values are means ± standard deviations.
Different capital letters (A–C) within the same column indicate significant differences between groups by one-way analysis of variance with Bonferroni *post-hoc* test ($p<0.05$).
Different lowercase letters (a–d) within the same row indicate significant differences between bleaching time points by one-was analysis of variance with Bonferroni *post-hoc* test ($p<0.05$).

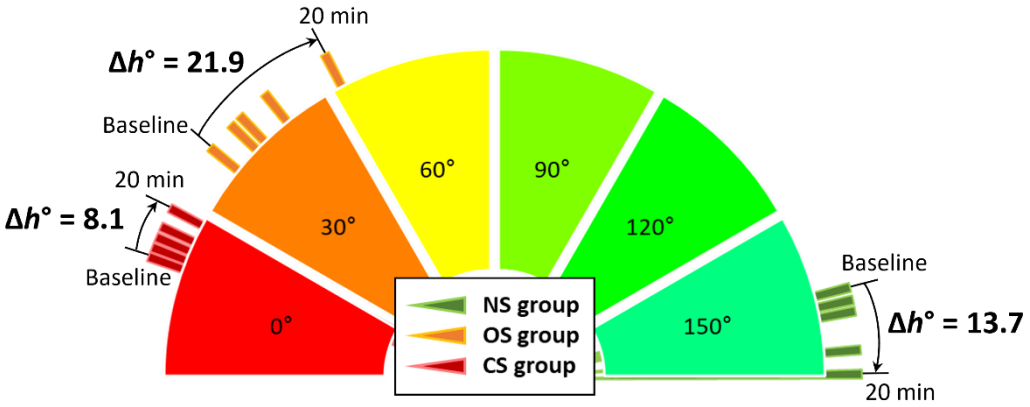

Figure 15. Changes in the biofluorescence hue angles (*h*°) of caries lesion parts with respect to bleaching time for each group (n = 10 in each group).

Δ*h*° values indicate differences in *h*° values between after 20 min of bleaching and before bleaching ($\Delta h^\circ = h^\circ_{20min} - h^\circ_{Baseline}$).
NS, non-stained; OS, organic-stained; CS, cariogenic-stained lesion group.

3.1.4. Hyperspectral biofluorescence spectra

The normalized BF spectrum was used to compare the BF color changes emitted from the discolored lesions at various wavelengths before and after bleaching when irradiated by a 405 nm light source (Figure 16). Before bleaching, the CS and OS groups showed their first emission peaks at 513 nm and 519 nm, respectively, in the blue-green region (460–560 nm). These peaks were shifted to the right compared to the 486 nm peak of sound enamel. In contrast to the OS group, which exhibited a single peak, the CS group demonstrated a second emission peak in the red region (620–780 nm). After 10 and 20 minutes of bleaching, the wavelengths of the first peak for the CS and OS groups were approximately 510 nm and 490 nm, respectively. These peaks shifted towards the direction of the sound enamel peak (left) as the bleaching time increased. The second red peak of the CS group showed a tendency to decrease in intensity, but it was clearly observed to persist even after 20 minutes of bleaching. In the NS group, the wavelength of the emission peak and the BF spectrum were similar to those of sound enamel at all time points before and after bleaching.

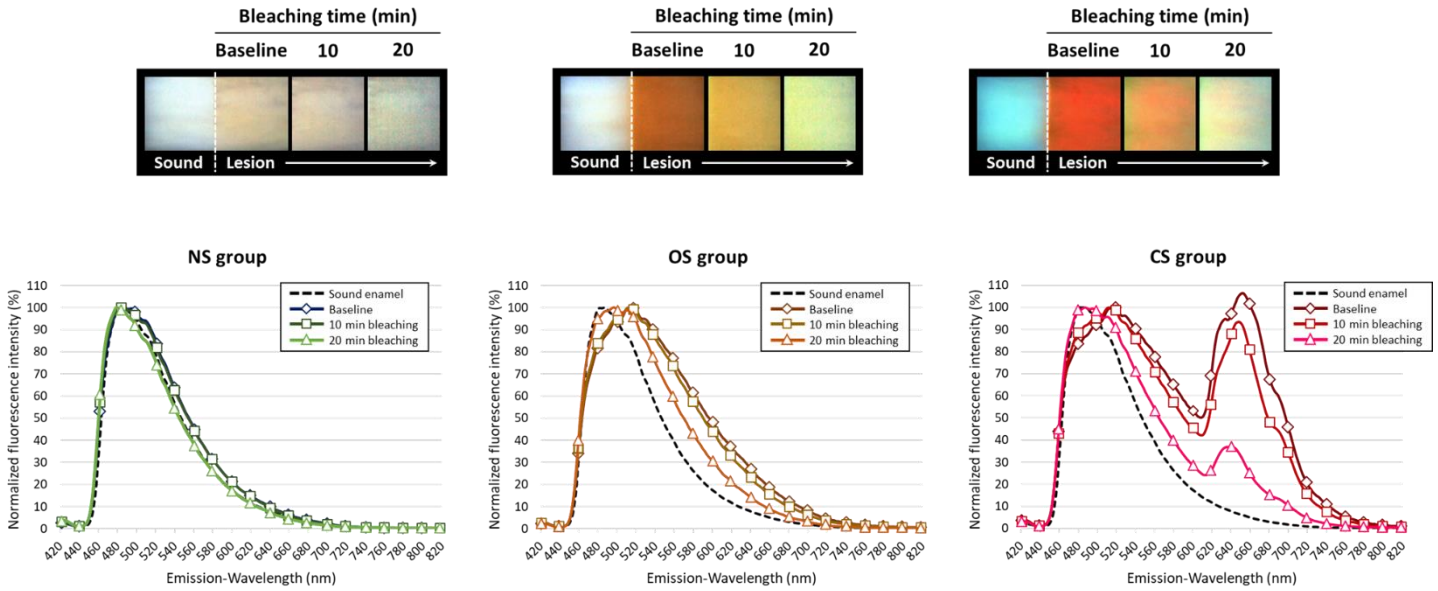

Figure 16. Biofluorescence emission spectra with respect to bleaching time for non-stained (NS), organic-stained (OS), and cariogenic-stained (CS) groups at 405 nm excitation using hyperspectral imaging (n = 10 in each group).

The dotted line indicates the reference spectrum of sound enamel for comparison with the lesion area.
NS, non-stained; OS, organic-stained; CS, cariogenic-stained lesion group.

3.2. Changes in biofluorescence properties of the cariogenically discolored pit and fissure after dental bleaching (study 2)

Through histological evaluation, a total of 69 teeth were finally used in the analysis out of a collective pool of 93 teeth. Excluded teeth included three teeth damaged during the preparation of histological samples and 21 teeth in which external debris was not removed from the evaluation area due to deep pits and fissures. According to histological criteria, the distribution of caries severity in the teeth used for the study showed 9 sound teeth, 34 enamel caries, and 17 dentin caries. When enamel caries were classified by lesion depth, 14 lesions were classified as E1 and 30 lesions as E2 (Table 6).

3.2.1. Visual and radiographic examination

A cross-table of ICDAS-II and radiographic examination results, based on the corresponding histological criteria, was presented in Table 6. In the visual inspection results using ICDAS-II, there were 17 sound teeth, 29 enamel caries (code 1: 15, code 2: 14), and 23 dentin caries (code 3: 13, code 4: 10). On the other hand, the radiographic examination results showed 48 sound teeth, 12 enamel caries, and 9 dentin caries. When compared with histological evaluation results, the correlation coefficients between ICDAS-II and radiographic examination were 0.66 and 0.55, respectively, indicating a moderate level of correlation.

Table 6. Cross-tabulation for the visual and radiographic examination of discolored occlusal caries with the corresponding histology scores.

Histological score	ICDAS-II					Radiography			Total (%)
	0	1	2	3	4	0	1	2	
S	8					8			8 (11.6)
E1	4	8	2			14			14 (20.3)
E2	5	6	8	4	7	20	9	1	30 (43.5)
D		1	4	9	3	6	3	8	17 (24.6)
Total (%)	17 (24.6)	15 (21.7)	14 (20.3)	13 (18.8)	10 (14.5)	48 (69.6)	12 (17.4)	9 (13.0)	69 (100.0)
Spearman's rho (ρ)			0.66**					0.55**	

S, sound; E1, demineralization in outer enamel; E2, demineralization in inner enamel; D, demineralization in outer dentin.
ICDAS-II, international caries detection and assessment system.
** $p<0.01$.

3.2.2. Distribution of histology and cariogenic discoloration

In order to classify cariogenic discoloration existing on the occlusal surfaces of the assessed teeth, each occlusal pit and fissure was designated as an individual analytical unit for evaluation. Following histological assessment of each pit and fissure, a total of 197 sites were assessable from 69 teeth. Out of a total of 197 pits and fissures, 30 were classified as sound, 135 exhibited enamel caries, and 32 showed dentin caries (Table 7). Upon further segmentation based on the depth of enamel caries lesions, 59 were categorized as E1 lesions, while 76 were classified as E2 lesions. When distinguishing cariogenic discoloration based on the histological results and the presence or absence of red BF observed in the pits and fissures before bleaching, there were 30 Sound, 62 Non-RF, and 105 RF cases.

Table 7. Cross-tabulation for the cariogenic discoloration with the corresponding histology scores.

Histological score	Number of discolored pit and fissure			Total (%)
	Sound	Non-RF	RF	
S	30	0	0	30 (15.2)
E1	0	13	46	59 (29.9)
E2	0	32	44	76 (38.6)
D	0	17	15	32 (16.2)
Total (%)	30 (15.2)	62 (31.5)	105 (53.3)	197 (100.0)

S, sound; E1, demineralization in outer enamel; E2, demineralization in inner enamel; D, demineralization in outer dentin.
Non-CD, noncariogenic discoloration; CD-non-RF, cariogenic discoloration with no red biofluorescence; CD-RF, cariogenic discoloration with red biofluorescence.

3.2.3. Color changes of discolored lesion area in the white-light image

Upon observation of the white-light images, all groups exhibited pits and fissures appearing as dark brown, and the three groups were indistinguishable, leading to an inability to differentiate between the Sound, Non-RF, and RF groups (Figure 17). As bleaching progressed, the discolored pits and fissures showed a gradual lighting in color across all lesion types. Additionally, in the Non-RF and RF groups, a white-to-brown opacity was observed within the pit and fissure area.

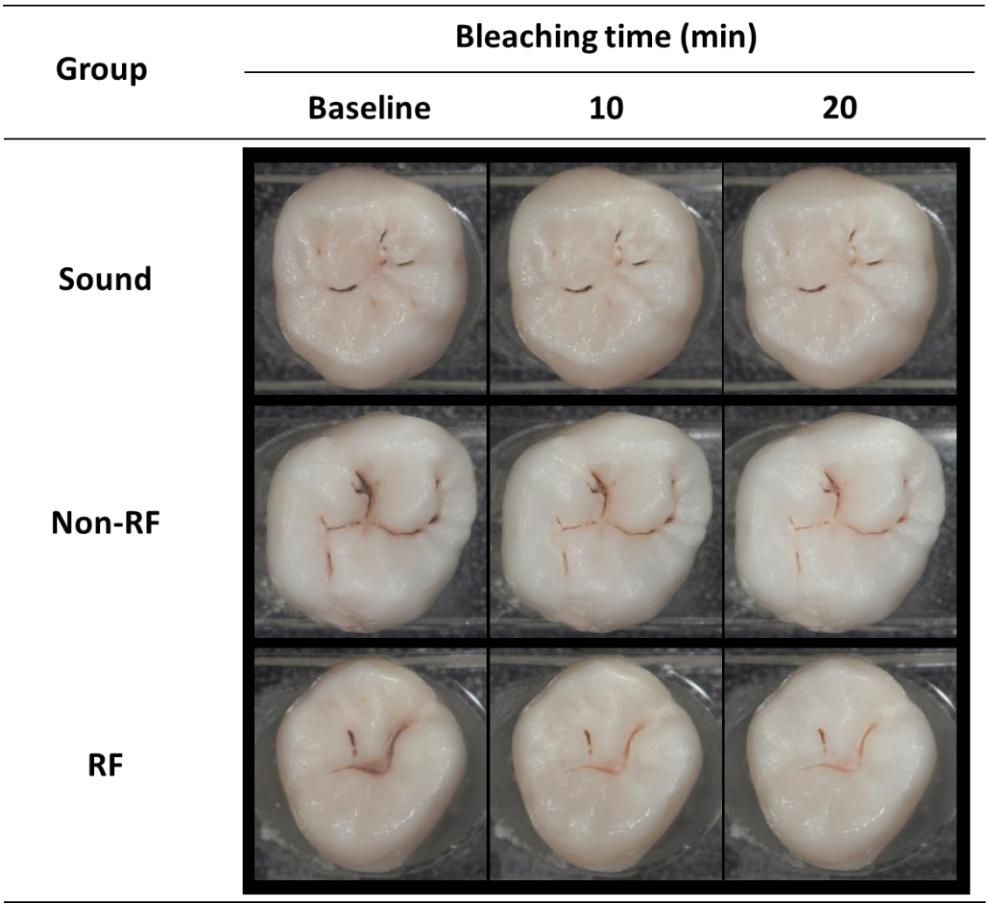

Figure 17. Representative white-light images of discolored pit and fissure for each group in relation to the duration of dental bleaching.

Sound, noncariogenic discoloration; Non-RF, cariogenic discoloration with no red biofluorescence; RF, cariogenic discoloration with red biofluorescence.

3.2.4. Changes in red biofluorescence intensity of cariogenic discoloration

Upon observation of the BF images, both the Sound and Non-RF groups exhibited pits and fissures displaying dark brown BF. In the RF group prior to bleaching, dark red BF was observed in the pits and fissures, whereas no red BF was observed in the Sound and Non-RF groups (Figure 18). Sound enamel in all groups showed green BF. As bleaching progressed, a trend of brightening BF in the pits and fissures was observed, and in the Non-RF group, the dark brown BF transformed into red BF. The results of calculating the ratio of the red BF intensity of the lesion to the sound enamel in the BF images showed that the ΔR values of the three groups before bleaching were significantly different ($p<0.001$, Table 8). However, from 5 minutes after bleaching, there was no significant difference between the Non-RF and RF groups. The ΔR value of the Non-RF group increased by approximately 15% compared to the baseline after 5 minutes bleaching, showing a significant difference ($p<0.001$). However, there was no difference observed up to 20 minutes after bleaching (Figure 19). In contrast, the red BF intensity of the Sound and RF groups did not show any significant changes at any bleaching time points.

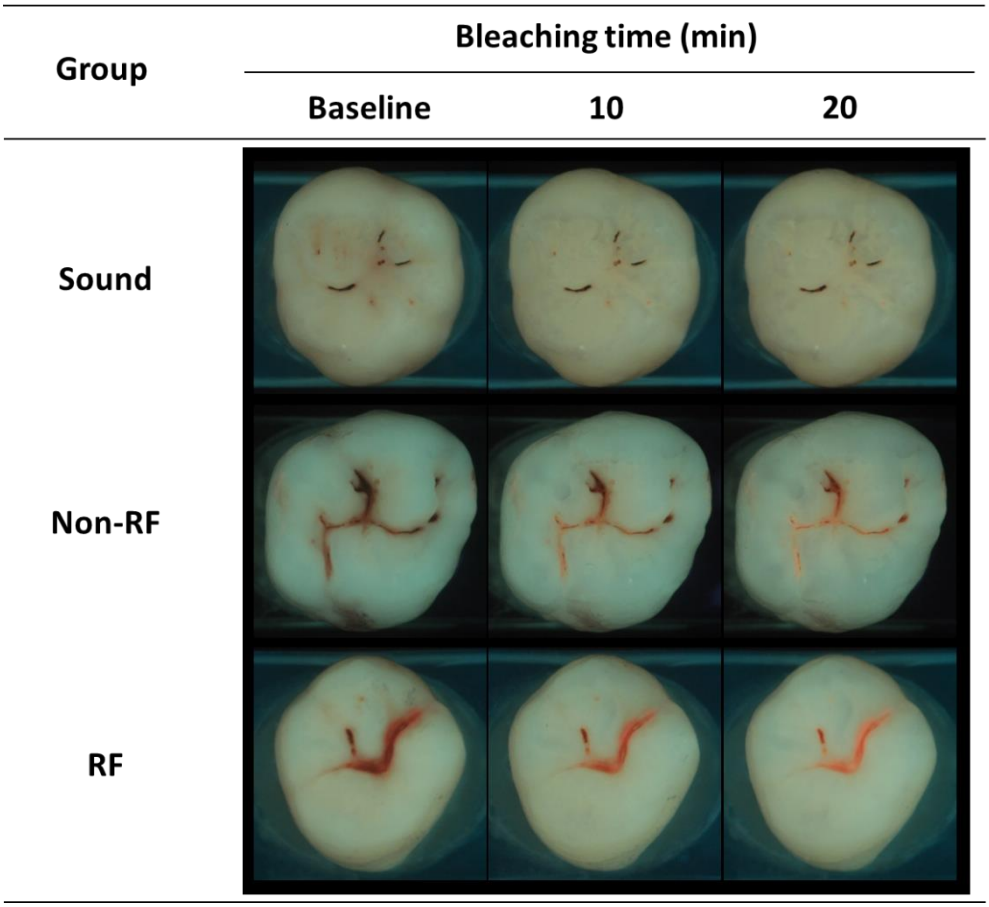

Figure 18. Representative BF images of discolored pit and fissure for each group in relation to the duration of dental bleaching.

Sound, noncariogenic discoloration; Non-RF, cariogenic discoloration with no red biofluorescence; RF, cariogenic discoloration with red biofluorescence.

Table 8. Differences in red biofluorescence intensity (Δ*R*) of discolored pit and fissure for each group, with respect to bleaching time.

Δ*R* (%) Groups	*n*	Bleaching time (min)				
		Baseline	5	10	15	20
Sound	30	31.50 [A, a] (29.30, 37.03)	32.20 [A, a] (28.18, 37.45)	32.05 [A, a] (28.43, 38.53)	32.75 [A, a] (27.53, 38.35)	31.90 [A, a] (27.78, 41.88)
Non-RF	62	40.95 [B, a] (35.88, 47.08)	47.00 [B, b] (40.25, 54.68)	48.60 [B, b] (41.30, 56.70)	49.95 [B, b] (42.98, 57.23)	51.50 [B, b] (44.00, 61.58)
RF	105	46.70 [C, a] (39.40, 63.60)	48.40 [B, a] (39.55, 62.50)	46.60 [B, a] (37.75, 58.60)	46.50 [B, a] (37.95, 58.55)	45.20 [B, a] (16.00, 27.50)

Data are median (first, third quartile) values.
Different capital letters (A–C) within the same column indicate significant differences between groups by the Kruskal-Wallis test and Mann-Whitney test with Bonferroni *post-hoc* correction.
Different lowercase letters (a–b) within the same row indicate significant differences between bleaching time points by the Kruskal-Wallis test and Mann-Whitney test with Bonferroni *post-hoc* correction.
Sound, noncariogenic discoloration; Non-RF, cariogenic discoloration with no red biofluorescence; RF, cariogenic discoloration with red biofluorescence.

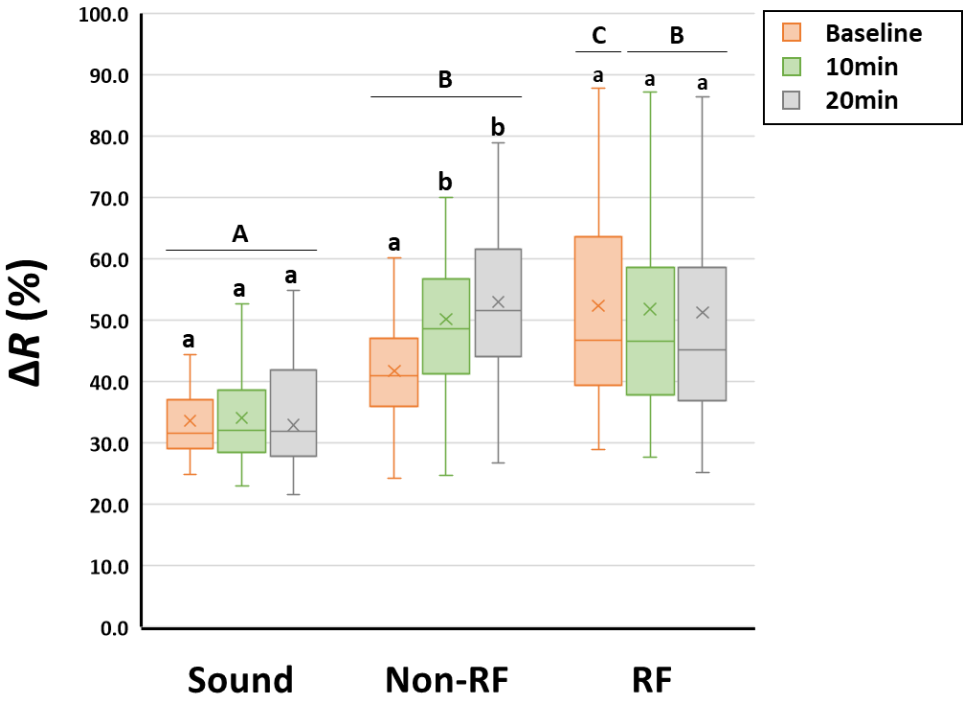

Figure 19. Changes in the red biofluorescence intensity (Δ*R*) with respect to bleaching time for noncariogenic discoloration (Sound), cariogenic discoloration with no red biofluorescence (Non-RF), and cariogenic discoloration with red biofluorescence (RF) groups.

Different capital letters (A–C) within the same column indicate significant differences between groups by the Kruskal-Wallis test and Mann-Whitney test with Bonferroni *post-hoc* correction.
Different lowercase letters (a–b) within the same row indicate significant differences between bleaching time points by the Kruskal-Wallis test and Mann-Whitney test with Bonferroni *post-hoc* correction.

3.2.5. Changes in biofluorescence hue angle of cariogenic discoloration

By analyzing the $h°$ values to determine the hue range of the discolored pits and fissures at the baseline, it was found that the BF hue emitted by the RF group was located in the red range. In contrast, the Sound and Non-RF groups displayed BF hues in the orange range. The $h°$ values of the three groups differed significantly before bleaching ($p<0.001$). However, from 5 minutes after bleaching, there was no significant difference between the Non-RF and RF groups (Table 9). As the bleaching time progressed, the $h°$ values of the Non-RF group decreased, while the $h°$ values of the Sound and RF groups increased. Twenty minutes after bleaching, the $h°$ value of the Non-RF group decreased by 2.05° compared to the baseline, which was not statistically significant, but hue range shifted from orange (15–45°) to red (345–15°) (Figure 20). In contrast, the $h°$ value of the RF group significantly increased by approximately 2.00° after 20 minutes of bleaching ($p<0.001$), but it remained within the same red range.

Table 9. Differences in biofluorescence hue angle (*h*°) of discolored pit and fissure for each group, with respect to bleaching time.

h° (degree) Groups	*n*	Bleaching time (min)				
		Baseline	5	10	15	20
Sound	30	20.85 [A, a] (17.70, 23.85)	23.10 [A, a] (20.13, 26.00)	23.50 [A, a] (18.83, 26.25)	23.40 [A, a] (18.60, 27.20)	24.10 [A, a] (19.28, 28.70)
Non-RF	62	17.50 [B, a] (13.58, 21.15)	17.45 [B, a] (13.55, 20.10)	16.15 [B, a] (12.88, 19.40)	15.40 [B, a] (12.88, 19.63)	15.45 [B, a] (12.88, 19.05)
RF	105	13.60 [C, a] (10.40, 16.40)	15.70 [B, b] (12.70, 18.30)	15.70 [B, b] (12.80, 19.20)	15.40 [B, b] (12.25, 19.30)	15.60 [B, b] (16.00, 27.50)

Data are median (first, third quartile) values.
Different capital letters (A–C) within the same column indicate significant differences between groups by the Kruskal-Wallis test and Mann-Whitney test with Bonferroni *post-hoc* correction.
Different lowercase letters (a–b) within the same row indicate significant differences between bleaching time points by the Kruskal-Wallis test and Mann-Whitney test with Bonferroni *post-hoc* correction.
Sound, noncariogenic discoloration; Non-RF, cariogenic discoloration with no red biofluorescence; RF, cariogenic discoloration with red biofluorescence.

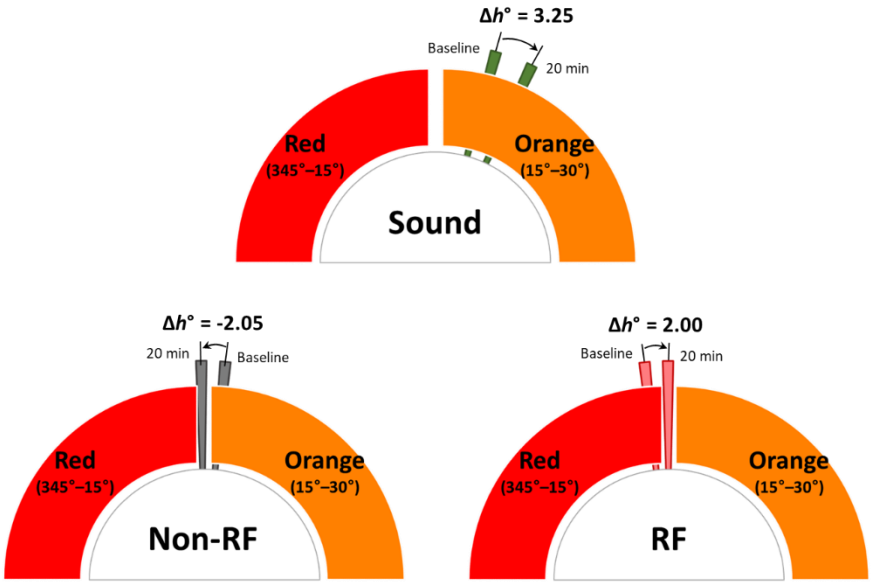

Figure 20. Changes in the biofluorescence hue angle (*h*°) with respect to bleaching time for noncariogenic discoloration (Sound), cariogenic discoloration with no red biofluorescence (Non-RF), and cariogenic discoloration with red biofluorescence (RF) groups.

Different capital letters (A–C) within the same column indicate significant differences between groups by the Kruskal-Wallis test and Mann-Whitney test with Bonferroni *post-hoc* correction.
Different lowercase letters (a–b) within the same row indicate significant differences between bleaching time points by the Kruskal-Wallis test and Mann-Whitney test with Bonferroni *post-hoc* correction.

3.3. Diagnostic performance of biofluorescence parameters for distinguishing cariogenic discoloration (study 2)

3.3.1. Changes in diagnostic performance of red biofluorescence intensity

The ΔR parameter was evaluated at different bleaching time points for its ability to distinguish between the Sound and Non-RF groups, which were difficult to differentiate due to the absence of red BF in all discolored pits and fissures before bleaching (Table 10). The ability of ΔR to distinguish Non-RF showed an improvement in specificity from 0.70 to 0.80 and in sensitivity from 0.79 to 0.90 before bleaching and 5 minutes after bleaching. The AUROC values were high, exceeding 0.77 at all bleaching time points. The sensitivity of ΔR for distinguishing the cariogenic discolored group (including Non-RF and RF groups, collectively referred to as the CD groups) was 0.84 both before and 5 minutes after bleaching, while the specificity improved from 0.70 to 0.83. AUROC values were above 0.84 at all time points. In both the Non-RF group and CD groups, specificity increased 5 minutes after bleaching compared to baseline, with the maximum AUROC value reaching 0.89. At the other bleaching time points, there were no significant changes in AUROC values for either the Non-RF group or CD groups.

Table 10. Sensitivity, specificity, area under receiver operating characteristics (AUROC) curve of red biofluorescence intensity (Δ*R*) for detecting cariogenic discoloration with respect to bleaching time.

Cutoff		Bleaching time (min)				
		Baseline	5	10	15	20
Sound vs. Non-RF	Sensitivity	0.79	0.90	0.84	0.89	0.90
	Specificity	0.70	0.80	0.80	0.77	0.73
	AUROC (S.E)	0.77 (0.05)	0.89 (0.04)	0.88 (0.04)	0.88 (0.04)	0.89 (0.03)
Sound vs. CD†	Sensitivity	0.84	0.84	0.76	0.80	0.86
	Specificity	0.70	0.83	0.80	0.77	0.73
	AUROC (S.E)	0.84 (0.04)	0.89 (0.03)	0.85 (0.04)	0.85 (0.04)	0.85 (0.04)

Sound, noncariogenic discoloration; CD, cariogenic discoloration; Non-RF, cariogenic discoloration with no red biofluorescence; RF, cariogenic discoloration with red biofluorescence.
CD† consists of the Non-RF and RF groups.
SE, standard error.

3.3.2. Changes in diagnostic performance of biofluorescence hue angle

Excluding the RF group, the AUROC value of $h°$ for distinguishing between the Sound and Non-RF groups was the lowest before bleaching at 0.69, but it was the highest at 0.93 five minutes after bleaching (Table 11). Furthermore, the sensitivity increased five minutes after bleaching, remained above 0.60, and reached the highest value of 0.92 twenty minutes after bleaching. The specificity was also above 0.67 at all bleaching time points, rising to over 0.90 at 10 and 15 minutes after bleaching. When evaluating the ability of $h°$ to distinguish the CD groups in all discolored pits and fissures, the AUROC value was highest at 0.87 five minutes after bleaching and remained above 0.84 at other bleaching time points. Up to five minutes after bleaching, a balance between sensitivity and specificity was observed in both the Non-RF group and CD groups. However, after ten minutes of bleaching, an imbalance between these two factors was observed, while the AUROC values did not show significant changes.

Table 11. Sensitivity, specificity, area under receiver operating characteristics (AUROC) curve of biofluorescence hue angle (*h*°) for detecting cariogenic discoloration with respect to bleaching time.

Cutoff		Bleaching time (min)				
		Baseline	5	10	15	20
Sound vs. Non-RF	Sensitivity	0.60	0.77	0.60	0.63	0.92
	Specificity	0.73	0.77	0.93	0.90	0.67
	AUROC (S.E)	0.69 (0.06)	0.93 (0.02)	0.83 (0.04)	0.84 (0.04)	0.86 (0.04)
Sound vs. CD†	Sensitivity	0.77	0.75	0.67	0.64	0.90
	Specificity	0.73	0.87	0.90	0.90	0.67
	AUROC (SE)	0.81 (0.04)	0.87 (0.03)	0.85 (0.04)	0.84 (0.04)	0.86 (0.04)

Sound, noncariogenic discoloration; CD, cariogenic discoloration; Non-RF, cariogenic discoloration with no red biofluorescence; RF, cariogenic discoloration with red biofluorescence.
CD† consists of the Non-RF and RF groups.
SE, standard error.

IV. Discussion

The present study investigated the changes in tooth BF resulting from bleaching discolored pits and fissures that are difficult to distinguish. By comparing the BF color changes induced by bleaching, we evaluated the stains associated with caries to organic stains within the discolored lesions. Additionally, after removing organic stains through bleaching, we evaluated whether the BF parameters could identify cariogenic discoloration from the discolored pits and fissures. To the best our knowledge, there are no previous studies that have detected caries using BF color information after applying bleaching to discolored teeth. Furthermore, this study is the first to attempt the BF-bleaching method to differentiate cariogenic discoloration from sound teeth by utilizing BF characteristics that vary according to the type of discoloration, aiming to identify cariogenic discoloration that is difficult to detect before bleaching.

In the first study, we artificially simulated cariogenic discoloration involving both bacterial fluorescing porphyrin and organic staining. After removing the organic stains through bleaching, we applied the BF-bleaching method to measure the BF color changes. In the second study, we applied the BF-bleaching method to extracted teeth with discolored pits and fissures and used the BF color changes to differentiate cariogenic discoloration. As a result, we found that when bleaching discolored pits and fissures, the organic stains within the cariogenically discolored lesions were removed first, while the characteristics of the red BF were maintained.

The present study used BF imaging to distinguish various discolored lesions that are difficult to differentiate with the naked eye. When photographing artificially simulated lesion samples, both CS and OS lesions appeared as dark brown discolorations in the white-light images, making it impossible to distinguish between the two groups (Figure 12). After applying bleaching, both CS and OS lesions showed a tendency to lighten to a bright brown discoloration in the captured white-light images. However, it was still not possible to distinguish between the two groups with the naked eye. In the white-light images of the discolored pits and fissures of real teeth, all groups (Sound, Non-RF, and RF) exhibited brown-black discoloration, and it was not possible to distinguish between these groups (Figure 17). As bleaching progressed, the color of the discolored pits and fissures in all three groups lightened. In the CD group, white-brown opacity was observed in the pits and fissures. This allowed the CD group to be distinguished from the Sound group, but it was not possible to differentiated between the Non-RF and RF within the CD group. In contrast, the BF images showed differences in the BF colors of each group. In the BF images of the simulation model, the CS group exhibited a dark red BF, while the OS group displayed a dark brown BF (Figure 13). As the bleaching time increased, the BF of both the CS and OS groups brightened; however, the BF colors of the two groups remained distinct. In the BF images of real teeth, the RF group exhibited a dark red BF, whereas the Sound and Non-RF groups displayed a dark brown BF (Figure 17). After the bleaching treatment, significant changes in BF were observed in the CD groups. In the Non-RF group, the brown BF disappeared and brightened, revealing a red BF. In the RF group, the red BF brightened

but was maintained. As a result, it was possible to distinguish cariogenic discoloration from sound teeth based on the presence of red BF before and after bleaching. Therefore, we confirmed the potential of using BF imaging to distinguish between organic stains and cariogenic discoloration, which are difficult to differentiate with the naked eye, by observing the BF color changes before and after bleaching.

The simulation model of this study infiltrated Protoporphyrin IX, known as a metabolite of caries-related bacteria, along with organic staining material (coffee powder) into early caries lesions artificially formed to simulate red BF of bacterial origin expressed in real discolored caries lesions. A previous study observed the cut surface of the extracted tooth with the cariogenically discolored lesion using BF imaging, and confirmed that stains existed in the upper part of the lesion site and red BF was expressed in the lower part (Lee et al., 2018). In this way, the phenomenon in which BF of bacterial origin and organic staining factors were simultaneously observed in the real caries lesion was reproduced in the simulation model. As a result of applying bleaching to remove organic stains, which could cause confusion in observing lesions, it was confirmed that the organic stains were removed as the bleaching progressed over time, with the BF becoming brighter in both groups. In particular, in the OS group, which replicated only organic stained lesion, it was confirmed that the BF color changed from brown to yellow-green before and after bleaching. Through this, it was confirmed that the stained BF decreased and the natural green BF of the enamel was simultaneously expressed (Figure 13). In the CS group, red BF was maintained after bleaching, which is thought to express red BF because the porphyrin

inside the lesion remains without being removed by hydrogen peroxide. Based in the results of the Simulation model, when BF-bleaching was applied to real discolored teeth, the Sound and RF groups could be distinguished according to the presence or absence of red BF before bleaching (Figure 18), which was similar to the results of the previous study (Lee et al., 2018). However, the Non-RF group before bleaching was indistinguishable from Sound. As the bleaching time increased, organic stains were removed and red BF was expressed below, making it possible to identify the lesion as cariogenic discoloration. Therefore, this study evaluated the effect of bleaching on organic stains and red BF color change of bacterial origin under conditions that controlled external environment and influencing factors. The results confirmed that it was possible to utilize bleaching treatment to distinguish cariogenic discoloration.

This study calculated the ΔR value, a parameter commonly used in red BF evaluation, to compare the intensity of red BF expressed in discolored lesions. Typically, the ΔR parameter is used to evaluate caries-related lesions by quantifying the red BF intensity expressed when 405 nm of light is irradiated to the teeth as the difference in BF levels between sound teeth and caries lesions (Jung et al., 2018; Lee et al., 2018; Oh et al., 2022). In the simulation model, the ΔR value of the CS group was about 2.74 times higher and 1.73 times higher than that of the OS group before and after 20 minutes of bleaching ($p<0.001$, Figure 14), respectively, and there was a difference in red BF intensity between two groups. However, after 20 minutes of bleaching, the ΔR value of the OS group decreased by about 43% compared to baseline, and the ΔR value of the CS group decreased by about 64%. On

the other hand, in extracted teeth, the ΔR values before and after bleaching in the Sound and RF groups showed no significant changes (Figure 19). In the Non-RF group, the ΔR value significantly increased 5 minutes after bleaching ($p<0.001$), and after 20 minutes, the ΔR value increased by about 26% compared to the baseline. The pattern of change in the ΔR value was different between the simulation model and the extracted teeth. Considering that the real cariogenic discoloration was formed over a long period of time, it would be differences from the simulation model that was maximized and simulated over a short period of time. Nevertheless, it was confirmed in the CS group of the simulation model that red BF was observed after organic stains were removed from real cariogenic discolored teeth, and it is believed that the simulation model of this study properly reflected cariogenic discoloration.

In the BF images of the simulation model, BF color differences were clearly observed in the CS and OS groups both before and after bleaching (Figure 13), but it was confirmed that there is a limitation in quantifying these color differences with ΔR value. The reason for this is the limitation of the ΔR parameter based on the RGB color system. ΔR describes the red BF intensity as the ratio difference between the R (red) and G (green) values of the BF of caries lesions and sound teeth. In this study, the ΔR value of the OS group before bleaching was 75.59, and the ΔR value of the CD group 20 minutes after bleaching was similar at 75.12 (Table 4). Contrary to those results, when looking at the BF image, the OS group before bleaching expressed a dark brown BF, while the CS group 20 minutes after bleaching showed a bright red BF (Figure 13). Through this, we confirmed that BF color

may be different even if the ΔR value is similar. Considering that discolored lesions express not red but also other colors of BF, we judged that the ΔR parameter alone, which describes the intensity of red BF as a ratio of R and G values, has limitations in distinguishing between CS and OS.

We also additionally calculated and confirmed the green BF intensity based on RGB color, which is known to well reflect the severity and depth of caries lesion. In the simulation model results, although the caries lesion depth (mean lesion depth ± standard deviation; 35.45 ± 3.12 μm) was the same in all NS, OS, and CS groups, the green BF intensity before bleaching was significantly different in all groups (p<0.001, Appendix Table 1). However, as the bleaching time passed, the green BF intensity of the discolored lesion group continued to increase, and after 20 minutes, the values of $|\Delta F|$ in the OS and CS groups recovered to a level similar to that of the NS group. In real teeth, $|\Delta F|$ values showed significant differences in Sound, Non-RF, and RF groups at all bleaching time points (p<0.001), and at 20 minutes of bleaching, green BF was significantly increased in all three groups compared to baseline (p<0.001, Appendix Table 2). Previous studies have reported that even for lesions of the same depth, when staining substances penetrate, $|\Delta F|$ values are exaggerated. Accordingly, there is a possibility that the discolored lesion may be misevaluated as a more severe caries lesion (Amaechi and Higham, 2002; Lee et al., 2018). Therefore, it is thought that bleaching of discolored pits and fissures can compensate for the fatal error in which values are overestimated when evaluating discolored lesions, but it was difficult to distinguish the three groups clearly because they also use only green BF

information. Consequently, it was necessary to explore new BF parameters to distinguish CS using BF color differences.

In order to overcome the limitations of RGB color-based parameters, this study explored a new color evaluation index that can quantify the hue of various BFs. The CIE Lab color system can express color information as a^* (negative is green, positive is red) and b^* (negative is blue, positive is yellow) and brightness information as L^* (achromatic coordinate) parameters (Lee, 2014). Considering the disadvantage that all of the R, G, B parameters of the RGB color system include brightness information (black to white), in this study, hue angle ($h°$) combining a^* and b^* parameters was calculated to quantify only the hue of discolored lesions except for brightness information (L^*). $h°$ is expressed as a continuous circular coordinate of 360°, and this study was able to intuitively check the BF hue of discolored lesions through color region where the $h°$ value of each group was located, and evaluate minute changes through the movement of coordinates. The $h°$ value of the CS group of the simulation model and that of the RF group of the real teeth continued to maintain the red region before and after bleaching (Figure 15 and Figure 20), which means that applying bleaching to cariogenic discoloration removes organic stains and the red BF of porphyrin origin remains. On the other hand, in the simulation model, the $h°$ value of the OS group containing only organic stains moved significantly in the orange hue region as the bleaching time increased, and then moved to the yellow region, a different hue, in 20 minutes of bleaching (Figure 15). Therefore, it was confirmed that the organic stains were clearly removed after bleaching in the OS group, and the change in the large $h°$ value was

expressed as a shift in the hue color region. The structure of the chromophore in organic stains is believed to be easily broken down ty hydrogen peroxide (H_2O_2) due to its conjugated system, compared to porphyrin. This leads to the typical bleaching phenomenon where the structure is disrupted and the stain is removed (Kwon and Wertz, 2015). In the case of organic stains, during bleaching, the oxygen released by H_2O_2 undergoes oxidation reactions, breaking one or more double bonds in the carbon ring structure and chain structure of the organic chromophore, converting them into colorless hydroxyl groups (Kwon and Wertz, 2015). On the other hand, porphyrin consists of four pyrrole rings and generates energy in the form of fluorescence and reactive oxygen species (Glowacka-Sobotta et al., 2019; Menon et al., 1990). In the case of the RF group of real teeth, the $h°$ value decreased by 2.05 from the baseline after bleaching for 20 minutes, and the hue region shifted from orange to red. Therefore, it was confirmed that bleaching process applied in this study decomposed organic stains before porphyrin.

In this study, the color information of various types of BFs expressed before and after bleaching of the simulation model was segmented by emission wavelength of multiple sections, and then spectrum was drawn after photographing with a hyperspectral camera (Figure 16). In the hyperspectral imaging results, the CS group could be clearly distinguished from the OS group, and the criteria for classification were the presence or absence of a peak in the red area (620–780 nm) showing a difference in the BF spectrum of the two groups. In the CS group, the baseline BF spectrum showed a second peak at an emission wavelength of 652 nm, and the previous study has reported that the emission peak

region of Protoporphyrin IX is 633–701 nm (Lennon Á et al., 2023). Thus, this implies that the presence or absence of a second red peak can clearly distinguish cariogenic discoloration of bacterial porphyrin origin. In addition, as a result of analyzing the BF change according to the bleaching time in the spectrum, it was confirmed that the spectrum of the first peak of all lesion groups that moved to the right at the baseline point of time moved in the spectral direction of the sound enamel after bleaching. However, the BF intensity of the second emission peak derived from porphyrin in the BF spectrum of the CS group decreased sharply after 20 minutes of bleaching, but it was clearly confirmed that it remained in the red area. This is thought to be due to photodegradation of porphyrin, which was repeatedly exposed to a 405 nm light source during the BF imaging process (Hope et al., 2011). Nevertheless, in the CS group, the second emission peak of the spectrum existed even after bleaching, and through this, the BF color information of the hyperspectral spectrum is considered an optical indicator that can be used to clearly distinguish between OS and CS.

This study conducted ROC analysis to determine whether BF parameters improve the ability to distinguish cariogenic discoloration after bleaching the discolored lesions. When using histological criteria to differentiate between Sound and cariogenic discoloration in pits and fissures before bleaching, the red BF intensity parameter in this study demonstrated high validity, with an accuracy of over 0.77 for distinguishing both CD groups and Non-RF group. Notably, the specificity increased by more than 0.10 five minutes after bleaching, which is likely due to the influence of the red BF that emerged as the organic staining was

removed. The increase in AUROC five minutes after bleaching was similarly observed in the BF hue angle parameter. Before and after bleaching, the $|\Delta F|$ values decreased in both the RF and Non-RF groups, whereas the ΔR value of the RF group remained unchanged, and the ΔR value of the RF group increased. Additionally, the $h°$ of the RF group increased, while the $h°$ of the Non-RF group decreased. The specificity of the green BF intensity was high at 0.97, whereas the sensitivity was low at 0.58, indicating an imbalance between the two factors (Appendix Table 3). These results differed from those of the previous study that used the BF information to distinguish between the Sound group and CD groups. In this study, the specificity was similar at 0.92, but the sensitivity was higher at 0.80 (Lee et al., 2018). Twenty minutes after bleaching, the sensitivity was 0.74 and the specificity was 0.70, showing a balance between the two factors. Despite differences in sensitivity and specificity before and after bleaching, cariogenic discoloration could be distinguished with high validity at all time points. When distinguishing between Sound and Non-RF groups, the AUROC value was higher than 0.90. However, considering the potential for overestimation of green BF intensity (Amaechi and Higham, 2002; Lee et al., 2018) and the difficulty in intuitively assessing the green BF intensity of cariogenic discoloration in BF images, using green BF information alone has its limitations. Therefore, previous studies have recommended using red BF intensity, which indicates the degree of bacterial involvement, alongside green BF intensity to distinguish cariogenic discoloration (Lee et al., 2018). In BF images, the changes in red BF before and after bleaching can be intuitively observed. Considering the different patterns of changes in $|\Delta F|$, ΔR, and $h°$ parameters

before and after bleaching in RF and Non-RF lesions, it is necessary to use both green BF and red BF changes together when distinguishing cariogenic discoloration.

The simulation model planned in this study was to simulate organic stains that masks the red BF of bacterial porphyrin in real cariogenic discolored teeth. Following this, we aimed to differentiate between cariogenic discoloration and organic stains by first removing organic stains through bleaching and then observing changes in BF color. However, the artificial cariogenically stained lesion in our study exhibited dark red BF even before bleaching. Nonetheless, there were limitations in accurately replicating the black discoloration that masks the red BF in discolored pits and fissures of real teeth. Previously, some simulation models inducing discoloration in artificial caries lesions existed. These models induced orange/brown organic stains using coffee or tea, or formed gray/black metallic stains using metal substances (Al-Angari et al., 2019). These models solely describe lesions characterized by discoloration, thereby limiting their ability to replicate the genuine cariogenic discolored lesion wherein bacterial porphyrin is implicated. On the other hand, this study devised the first cariogenic discoloration model that reflects the actual state of discolored caries by incorporating both porphyrin and organic stains into artificial caries lesions. This is meaningful in that OS and CS, which are difficult to distinguish with the naked eye, are divided by color comparison using BF imaging technology. In addition, it is significant that BF-bleaching was applied to discolored pits and fissures of real teeth, and by comparing the results with the simulation model, a new phenomenon associated with bleaching cariogenic discoloration was discovered.

This study is the first to differentiate cariogenic discoloration while removing organic stains using BF-bleaching method. In the simulation model of this study, the discolored lesion areas of the OS and CS groups with incorporated staining substances became lighter, reducing the color difference from sound enamel (p<0.001, Appendix Table 4) (Al-Angari et al., 2019; Kwon et al., 2015; Lee et al., 2019). Although there was a significant color difference between the two groups after 20 minutes of bleaching (p<0.001), these differences were not discernible in real clinical practice (Rutkūnas et al., 2020). When evaluating the real discolored pits and fissures of extracted teeth, the color of the Sound and CD groups was similar at all time points before and after bleaching. Although the Non-RF group had significantly higher values than the other two groups (Appendix Table 5), it was difficult to distinguish all groups visually. Furthermore, visual assessment using ICDAS-II and radiographic examination showed moderate correlations with histological examination, with correlation coefficients of 0.66 and 0.55, respectively (p<0.01, Table 8). Therefore, using color differences for visual inspection, as well as traditional methods, to distinguish cariogenic discoloration in discolored pits and fissures had limitations. In contrast, the BF-bleaching method allows clinicians to more objectively diagnose and monitor caries lesions by preferentially removing organic stains from discolored lesions that are difficult to distinguish. In addition, this method improves the aesthetics of discolored areas and aids in determining preventive and therapeutic options for discolored lesions. Moreover, in this study, red BF intensity and hue angle enhanced the ability to distinguish cariogenic discoloration from five minutes after bleaching. Utilizing various

light sources and photocatalytic materials in the bleaching process with hydrogen peroxide could further reduce the bleaching application time. In addition, this approach could reduce side effects associated with excessive bleaching, such as tooth sensitivity, surface morphological changes, and demineralization (Al-Angari et al., 2021; Lee et al., 2019; Yang et al., 2022), thereby enhancing the bleaching effect while quickly capturing the red BF of porphyrins. Utilizing the phenomenon, the BF-bleaching method could be applied not only discolored pits and fissures but also to various areas such as brown spots and the margins of discolored restorations. If further academic evidence for the BF-bleaching method's efficacy in distinguishing cariogenic discoloration is obtained in real clinical settings, this method could be effectively used as a theragnostic approach for identifying caries lesions.

V. Conclusions

The present study proposes BF-bleaching as a method to distinguish cariogenic discoloration in discolored pits and fissures. Bleaching was applied to discolored pits and fissures, and changes in BF parameters according to the type of discoloration were evaluated before and after bleaching. Additionally, this study aimed to determine whether the ability of the BF-bleaching method to distinguish cariogenic discoloration is enhanced by examining the patterns of change in BF parameters.

1. Applying BF-bleaching to the simulation model that mimicked cariogenic discoloration, the red BF intensity was highest in the CS group. Both before and after bleaching, the BF hue and spectrum peak of the CS group remained in the red region. In contrast, the hue of the OS group shifted from the orange to the yellow region, and there was no spectrum peak in the red region. These results suggest that, when bleaching discolored lesions, the presence or absence of hue and BF spectrum peaks in the red region can potentially be used to distinguish cariogenic discoloration.

2. When evaluating real discolored pits and fissures, there was no color difference between the Sound group and the RF group that exhibited red BF before bleaching. The red BF intensity in the Non-RF group, where no res BF was observed before bleaching, was low initially but increased after bleaching, becoming similar to that of the RF group. The BF hue angle of the Non-RF group shifted from the orange to the red region before and after bleaching. In contrast, the BF hue of the Sound group remained in the orange

region and the RF group in the red region, both before and after bleaching, maintaining their respective hue regions. Therefore, the Sound and cariogenic discoloration could be distinguished through red BF intensity, and the presence of Non-RF lesion, which is easy to overlook, was identified by changes in BF hue angle before and after bleaching.

3. ROC analysis was used to evaluate the ability of each BF parameter to distinguish cariogenic discoloration. Red BF intensity and BF hue angle showed improved ability to distinguish cariogenic discoloration five minutes after bleaching. After bleaching, all BF parameters demonstrated high validity in distinguishing cariogenic discoloration.

In conclusion, the discoloration of pit and fissures, which is difficult to distinguish visually, exhibited different BF characteristics depending on the type. The changes in BF color after bleaching allowed for the distinction of cariogenic discoloration. Specifically, the red BF associated with cariogenic discoloration is a key characteristic for distinguishing between cariogenic discoloration and sound teeth. Tooth bleaching helps to remove organic stains from discolored lesions and reveals the underlying red BF, thereby aiding in the identification of cariogenic discoloration. Therefore, BF-bleaching can be a promising method in clinical practice for objectively distinguishing cariogenic discoloration and for tracking caries lesions in discolored pits and fissures.

References

Abu-Hanna A, Mjör IA (2008). Stain vs caries. *Oper Dent* 33(1): 108-110.

Al-Angari SS, AlHadlaq M, Abahussain N, AlAzzam N (2021). Bleaching Stained Arrested Caries Lesions: In vivo Clinical Study. *Eur J Dent* 15(1): 127-132.

Al-Angari SS, Hara AT (2016). A conservative approach to esthetically treat stained arrested caries lesions. *Quintessence Int* 47(6): 499-504.

Al-Angari SS, Lippert F, Platt JA, Eckert GJ, González-Cabezas C, Li Y, Hara AT (2019). Dental bleaching efficacy and impact on demineralization susceptibility of simulated stained-remineralized caries lesions. *J Dent* 81: 59-63.

Amaechi BT, Higham SM (2002). Quantitative light-induced fluorescence: a potential tool for general dental assessment. *J Biomed Opt* 7(1): 7-13.

Carvalho JC (2014). Caries process on occlusal surfaces: evolving evidence and understanding. *Caries Res* 48(4): 339-346.

Carvalho JC, Dige I, Machiulskiene V, Qvist V, Bakhshandeh A, Fatturi-Parolo C, Maltz M (2016). Occlusal Caries: Biological Approach for Its Diagnosis and Management. *Caries Res* 50(6): 527-542.

Christensen RP, Ploeger BJ, Palmer TM (2001). The role of pit-and-fissure discoloration in caries assessment. *Compend Contin Educ Dent* 22(11a): 996-1002, 1004-1007; quiz 1044.

Côrtes DF, Ellwood RP, Ekstrand KR (2003). An in vitro comparison of a combined FOTI/visual

examination of occlusal caries with other caries diagnostic methods and the effect of stain on their diagnostic performance. *Caries Res* 37(1): 8-16.

Dikmen B (2015). Icdas II criteria (international caries detection and assessment system). *J Istanb Univ Fac Dent* 49(3): 63-72.

Falconer DS, Hamilton JC, Stoffers KW, Gregory WA (2008). Tooth bleaching and pit and fissure stain. *Am J Dent* 21(2): 71-73.

Glowacka-Sobotta A, Wrotynski M, Kryjewski M, Sobotta L, Mielcarek J (2019). Porphyrinoids in photodynamic diagnosis and therapy of oral diseases. *Journal of Porphyrins and Phthalocyanines* 23(01n02): 1-10.

Hakanson EC, Hakanson KJ, Anich PS, Martin JG (2022). Techniques for documenting and quantifying biofluorescence through digital photography and color quantization. *Journal of Photochemistry and Photobiology* 12: 100149.

Han SY, Kim BR, Ko HY, Kwon HK, Kim BI (2016). Assessing the use of Quantitative Light-induced Fluorescence-Digital as a clinical plaque assessment. *Photodiagnosis Photodyn Ther* 13: 34-39.

Hariri I, Sadr A, Nakashima S, Shimada Y, Tagami J, Sumi Y (2013). Estimation of the enamel and dentin mineral content from the refractive index. *Caries Res* 47(1): 18-26.

Hope CK, de Josselin de Jong E, Field MR, Valappil SP, Higham SM (2011). Photobleaching of red fluorescence in oral biofilms. *J Periodontal Res* 46(2): 228-234.

Jun MK, Park SW, Lee ES, Kim BR, Kim BI (2019). Diagnosis and management of cracked tooth by quantitative light-induced fluorescence technology. *Photodiagnosis Photodyn Ther* 26: 324-326.

Jung EH, Lee ES, Jung HI, Kang SM, de Josselin de Jong E, Kim BI (2018). Development of a fluorescence-image scoring system for assessing noncavitated occlusal caries. *Photodiagnosis Photodyn Ther* 21: 36-42.

Kapor S, Rankovic MJ, Khazaei Y, Crispin A, Schüler I, Krause F, et al. (2021). Systematic review and meta-analysis of diagnostic methods for occlusal surface caries. *Clin Oral Investig* 25(8): 4801-4815.

Kidd EA, Fejerskov O (2004). What constitutes dental caries? Histopathology of carious enamel and dentin related to the action of cariogenic biofilms. *J Dent Res* 83 Spec No C: C35-38.

Kim HE, Kwon HK, Kim BI (2009). Application of fluoride iontophoresis to improve remineralization. *J Oral Rehabil* 36(10): 770-775.

Kim SK, Jung HI, Kim BI (2020). Detection of dentin-exposed occlusal/incisal tooth wear using quantitative light-induced fluorescence technology. *J Dent* 103: 103505.

Kordic A, Lussi A, Luder HU (2003). Performance of visual inspection, electrical conductance and laser fluorescence in detecting occlusal caries in vitro. *Schweiz Monatsschr Zahnmed* 113(8): 852-859.

Kwon SR, Kurti SR, Jr., Oyoyo U, Li Y (2015). Effect of Light-Activated Tooth Whitening on Color Change Relative to Color of Artificially Stained Teeth. *J Esthet Restor Dent* 27 Suppl 1:

S10-17.

Kwon SR, Wertz PW (2015). Review of the Mechanism of Tooth Whitening. *J Esthet Restor Dent* 27(5): 240-257.

Lee ES, de Josselin de Jong E, Kim E, Kim BI (2023). Real-time optical detection of endodontic infection using bacterial autofluorescence. *J Dent* 136: 104600.

Lee HS, Kim SK, Park SW, de Josselin de Jong E, Kwon HK, Jeong SH, Kim BI (2018). Caries detection and quantification around stained pits and fissures in occlusal tooth surfaces with fluorescence. *J Biomed Opt* 23(9): 1-7.

Lee JY, Lee ES, Kang SM, Kim BI (2019). Application of quantitative light-induced fluorescence technology for tooth bleaching treatment and its assessment: An in vitro study. *Photodiagnosis Photodyn Ther* 25: 208-213.

Lee YK (2014). Correlation between three color coordinates of human teeth. *J Biomed Opt* 19(11): 115006.

Lennon Á M, Brune L, Techert S, Buchalla W (2023). Fluorescence Spectroscopy Shows Porphyrins Produced by Cultured Oral Bacteria Differ Depending on Composition of Growth Media. *Caries Res* 57(1): 74-86.

Lussi A (1993). Comparison of different methods for the diagnosis of fissure caries without cavitation. *Caries Res* 27(5): 409-416.

Mazel C (2017). Method for Determining the Contribution of Fluorescence to an Optical Signature,

with Implications for Postulating a Visual Function. *Frontiers in Marine Science* 4.

Mendes FM, de Oliveira E, de Faria DL, Nicolau J (2006). Ability of laser fluorescence device associated with fluorescent dyes in detecting and quantifying early smooth surface caries lesions. *J Biomed Opt* 11(2): 024007.

Menon IA, Becker MA, Persad SD, Haberman HF (1990). Quantitation of hydrogen peroxide formed during UV-visible irradiation of protoporphyrin, coproporphyrin and uroporphyrin. *Clin Chim Acta* 186(3): 375-381.

Oh SH, Choi JY, Kim SH (2022). Evaluation of dental caries detection with quantitative light-induced fluorescence in comparison to different field of view devices. *Sci Rep* 12(1): 6139.

Park SW, Kang SM, Lee HS, Kim SK, Lee ES, Kim BR, et al. (2022). Lesion activity assessment of early caries using dye-enhanced quantitative light-induced fluorescence. *Sci Rep* 12(1): 11848.

Park SW, Kim SK, Lee HS, Lee ES, de Josselin de Jong E, Kim BI (2019). Comparison of fluorescence parameters between three generations of QLF devices for detecting enamel caries in vitro and on smooth surfaces. *Photodiagnosis Photodyn Ther* 25: 142-147.

Pitts NB (1984). Systems for grading approximal carious lesions and overlaps diagnosed from bitewing radiographs. Proposals for future standardization. *Community Dent Oral Epidemiol* 12(2): 114-122.

Pretty IA (2006). Caries detection and diagnosis: novel technologies. *J Dent* 34(10): 727-739.

Rutkūnas V, Dirsė J, Bilius V (2020). Accuracy of an intraoral digital scanner in tooth color determination. *J Prosthet Dent* 123(2): 322-329.

Steiner M, Helfenstein U, Menghini G (1998). Association of salivary mutans streptococci with discoloured pits and fissures. *Community Dent Oral Epidemiol* 26(6): 412-417.

Walsh LJ, Shakibaie F (2007). Ultraviolet-induced fluorescence: shedding new light on dental biofilms and dental caries. *Australasian Dental Practice* 18(6): 56-60.

Watts A, Addy M (2001). Tooth discolouration and staining: a review of the literature. *Br Dent J* 190(6): 309-316.

White DJ (1987). Use of synthetic polymer gels for artificial carious lesion preparation. *Caries Res* 21(3): 228-242.

Yang SY, Choi JW, Kim KM, Kwon JS (2022). Effects of 35% hydrogen peroxide solution containing hydrated calcium silicate on enamel surface. *Clin Oral Investig* 26(2): 2133-2142.

Appendix Table 1. Differences in green biofluorescence intensity (|Δ*F*|, %) between sound enamel and caries lesion parts for each group, with respect to bleaching time (n = 10 in each group).

|Δ*F*| (%)	Bleaching time (min)				
Groups	Baseline	5	10	15	20
Non-stained (Negative control)	9.86 ± 3.43 $^{A, a}$	9.59 ± 3.02 $^{A, a}$	9.40 ± 3.67 $^{A, a}$	9.16 ± 3.24 $^{A, a}$	10.10 ± 3.60 $^{A, a}$
Organic-stained (Positive control)	48.10 ± 2.48 $^{B, a}$	32.12 ± 3.45 $^{B, b}$	22.57 ± 3.59 $^{B, c}$	14.09 ± 3.07 $^{B, d}$	8.59 ± 2.79 $^{A, e}$
Cariogenic-stained (Experimental group)	60.30 ± 3.23 $^{C, a}$	44.25 ± 4.28 $^{C, b}$	28.72 ± 5.90 $^{C, c}$	19.00 ± 6.09 $^{C, d}$	12.08 ± 5.69 $^{A, e}$

All values are means ± standard deviations.
Different capital letters (A–C) within the same column indicate significant differences between groups by one-way analysis of variance with Bonferroni *post-hoc* test ($p<0.05$).
Different lowercase letters (a–e) within the same row indicate significant differences between bleaching time points by one-was analysis of variance with Bonferroni *post-hoc* test ($p<0.05$).

Appendix Table 2. Differences in green biofluorescence intensity (|Δ*F*|) of discolored pit and fissure for each group, with respect to bleaching time.

|Δ*F*| (%) Groups	*n*	Bleaching time (min)				
		Baseline	5	10	15	20
Sound	30	20.40 [A, a] (15.65, 24.70)	17.45 [A, a ,b] (14.45, 22.85)	17.05 [A, a, b] (14.20, 22.78)	16.85 [A, a, b] (13.93, 21.50)	15.70 [A, b] (10.38, 18.38)
Non-RF	62	34.90 [B, a] (30.08, 39.98)	33.60 [B, a, b] (28.33, 38.35)	32.10 [B, a, b] (26.53, 37.03)	30.60 [B, a, b] (25.25, 37.05)	30.20 [B, b] (24.03, 35.90)
RF	105	25.80 [C, a] (21.40, 34.60)	24.20 [C, a, b] (19.75, 32.95)	22.60 [C, a, b, c] (18.30, 29.80)	22.20 [C, a, b, c] (17.05, 28.45)	21.70 [C, c] (16.00, 27.50)

Data are median (first, third quartile) values.
Different capital letters (A–C) within the same column indicate significant differences between groups by the Kruskal-Wallis test and Mann-Whitney test with Bonferroni *post-hoc* correction.
Different lowercase letters (a–c) within the same row indicate significant differences between bleaching time points by the Kruskal-Wallis test and Mann-Whitney test with Bonferroni *post-hoc* correction.
Sound, noncariogenic discoloration; Non-RF, cariogenic discoloration with no red biofluorescence; RF, cariogenic discoloration with red biofluorescence.

Appendix Table 3. Sensitivity, specificity, area under receiver operating characteristics (AUROC) curve of green biofluorescence intensity (|Δ*F*|) for detecting cariogenic discoloration with respect to bleaching time.

Cutoff		Bleaching time (min)				
		Baseline	5	10	15	20
Sound vs. Non-RF	Sensitivity	0.82	0.77	0.69	0.86	0.86
	Specificity	0.97	1.00	1.00	0.83	0.80
	AUROC (S.E)	0.92 (0.03)	0.93 (0.02)	0.92 (0.03)	0.91 (0.03)	0.90 (0.03)
Sound vs. CD†	Sensitivity	0.58	0.55	0.45	0.65	0.74
	Specificity	0.97	0.97	1.00	0.80	0.70
	AUROC (SE)	0.81 (0.04)	0.83 (0.03)	0.80 (0.04)	0.79 (0.04)	0.78 (0.04)

Sound, noncariogenic discoloration; CD, cariogenic discoloration; Non-RF, cariogenic discoloration with no red biofluorescence; RF, cariogenic discoloration with red biofluorescence.
CD† consists of the Non-RF and RF group.
SE, standard error.

Appendix Table 4. Color differences (ΔE^*) between sound enamel and caries lesion parts for each group, with respect to bleaching time (n = 10 in each group).

ΔE^*	Bleaching time (min)				
Groups	Baseline	5	10	15	20
Non-stained (Negative control)	4.69 ± 1.37 $^{A, a}$	4.57 ± 1.47 $^{A, a}$	4.75 ± 1.92 $^{A, a}$	4.81 ± 1.48 $^{A, a}$	4.22 ± 1.23 $^{A, a}$
Organic-stained (Positive control)	21.71 ± 1.42 $^{B, a}$	19.74 ± 1.42 $^{B, b}$	18.33 ± 1.20 $^{B, c}$	16.40 ± 1.13 $^{B, d}$	14.86 ± 1.54 $^{B, e}$
Cariogenic-stained (Experimental group)	23.15 ± 1.71 $^{B, a}$	21.65 ± 2.16 $^{B, b}$	18.25 ± 1.88 $^{B, c}$	15.97 ± 1.55 $^{B, d}$	12.95 ± 1.79 $^{C, e}$

All values are means ± standard deviations.
Different capital letters (A–C) within the same column indicate significant differences between groups by one-way analysis of variance with Bonferroni *post-hoc* test (p<0.05).
Different lowercase letters (a–e) within the same row indicate significant differences between bleaching time points by one-was analysis of variance with Bonferroni *post-hoc* test (p<0.05).

Appendix Table 5. Color differences (ΔE^*) of discolored pit and fissure for each group, with respect to bleaching time.

ΔE^*	n	Bleaching time (min)				
Groups		Baseline	5	10	15	20
Sound	30	15.95 $^{A, a}$ (14.28, 22.35)	15.00 $^{A, a}$ (13.45, 20.95)	15.20 $^{A, a}$ (12.20, 19.65)	13.95 $^{A, a}$ (11.88, 18.63)	12.95 $^{A, a}$ (10.38, 18.38)
Non-RF	62	24.95 $^{B, a}$ (20.78, 26.80)	24.45 $^{B, a}$ (19.93, 27.05)	23.25 $^{B, a}$ (18.63, 26.65)	23.10 $^{B, a}$ (17.90, 25.93)	22.50 $^{B, a}$ (16.78, 26.18)
RF	105	17.20 $^{A, a}$ (13.75, 21.75)	17.20 $^{A, a, b}$ (13.65, 22.00)	16.10 $^{A, a, b}$ (12.25, 20.55)	16.00 $^{A, a, b}$ (11.95, 20.25)	15.30 $^{A, b}$ (11.05, 19.95)

Data are median (first, third quartile) values.
Different capital letters (A–B) within the same column indicate significant differences between groups by the Kruskal-Wallis test and Mann-Whitney test with Bonferroni *post-hoc* correction.
Different lowercase letters (a–b) within the same row indicate significant differences between bleaching time points by the Kruskal-Wallis test and Mann-Whitney test with Bonferroni *post-hoc* correction.
Sound, noncariogenic discoloration; Non-RF, cariogenic discoloration with no red biofluorescence; RF, cariogenic discoloration with red biofluorescence.

ABSTRACT (IN KOREAN)

소와 열구의 우식성 변색 구분을 위한 생체형광-미백 적용법

<지도교수 김백일>

연세대학교 대학원 응용생명과학과

이형석

치아 교합면은 좁고 깊은 소와 열구를 가지고 있어 착색 물질이 부착하기 용이하며 치면세균막 등의 이물질 축적되기 쉽다. 교합면의 복잡한 해부학적 구조로 인하여 소와 열구로부터 외부 축적 물질을 제거하는 것은 어려우며, 이로 인해 교합면 우식이 발생하기 쉽다. 이 과정에서 탈회된 다공성 구조에 미생물과 함께 착색 물질의 발색단이 침투하면 갈색 또는 검은색 불투과성의 우식성 변색으로 진행된다. 소와 열구의 변색은 교합면 우식의 진단 결정에 영향을 미치는 요소 중 하나이며, 우식 여부를 판단하는 핵심적인 요인이다.

하지만 임상 현장에서 치과의사가 우식 과정에서 발생한 변색과 식품 색소와 같은 유기물에서 기인한 착색을 구분하는 것은 어렵다. 또한 교합면 우식의 진단 기준으로 변색을 사용하는 것은 여전히 논쟁의 여지가 있다.

치의학 분야에서 사용되고 있는 생체형광(BF) 기술은 단파장의 푸른색 가시광선을 치아에 조사하였을 때 발현되는 BF를 시각화하고 정량화하여 구강의 병적 상태를 평가한다. 치아 조직에서 발생하는 무기질 및 구조의 변화는 녹색 BF 강도 차이로, 구강 미생물의 대사 관련 병적 상태는 붉은 BF 강도로 확인할 수 있다. 실제로 BF를 사용하여 교합면의 우식성 변색을 구분하려는 노력은 있었다. 하지만 변색은 치아 표면을 마스킹하여 빛을 흡수하거나 산란시키기 때문에 변색된 교합면의 BF를 평가하는 것은 제한적이었다. 따라서 본 연구에서는 치아 미백 전후 변색된 소와 열구의 BF 색 변화를 확인하고, 우식성 변색 치아로부터 유기 착색을 제거한 뒤 교합면 우식을 탐지하는 방법으로서 BF-bleaching을 제안하고자 하였다.

본 연구는 크게 두 가지 실험으로 진행되었다. 첫 번째 연구는 우식성 변색을 모사한 simulation model에 BF-bleaching을 적용한 뒤 BF 색 변화를 비교하여 우식성 변색을 구분하고자 하였다. 두 번째 연구는 발치 치아의 변색 소와 열구에 BF-bleaching을 적용한 뒤 BF 색 변수들의 변화를 확인하고, 이를 통해 BF 색 변수들의 우식성 변색 구분 능력을 평가하고자 하였다.

첫 번째 연구에서는 우전치를 사용하여 우식성 변색에서 관찰되는 BF를 재현하여 평가하고자 착색 처치를 하지 않은 병소(NS), 유기 착색(OS), 우식성 변색(CS) 병소를 제작하였다. 착색을 제거하기 위해 미백 처치를 하였고, BF의 변화를 형광학적, 초분광학적으로 평가하였다. 미백으로 인해 착색이 제거될수록 병소의 BF는 밝아지는 경향을 보였지만, CS 군의 BF $h°$은 붉은색 영역(345°–15°)을 유지하였고, BF spectrum에서 붉은색 영역(620–780 nm)의 두번째 방출 peak도 명확하게 남아있었다. 반면 OS 군의 BF는 미백 후 주황(15°–45°)에서 노랑(45°–75°)으로의 뚜렷한 색조 변화가 있었지만, BF spectrum에서 붉은 영역의 두번째 방출 peak는 없었다.

두 번째 연구에서는 변색된 소와 열구가 존재하는 발치 치아에 미백을 적용하였고, BF의 색 변화를 개별적인 소와 열구 분석 단위로 평가하였다. 조직학적 평가 결과를 기반으로, 정상 부위인 비우식성 변색(Sound)과 우식성 변색(CD)을 구분하였다. 추가적으로 미백 전 BF 이미지의 교합면에서 관찰되는 붉은 BF의 존재 여부에 따라 우식성 변색을 더 상세하게 분류하였고, 이루 붉은 BF를 동반한 우식성 변색(RF)과 붉은 BF가 관찰되지 않는 우식성 변색(Non-RF)으로 구분하였다. 미백 전 Sound, Non-RF, RF 군의 붉은 BF 강도(ΔR)는 유의한 차이를 보였으나, 미백 5분 후에는 Non-RF와 RF 군의 ΔR 값이 유사하였다. 미백 후 BF $h°$은 RF 군에서 붉은색 영역, Sound 군에서 주황색 영역을 유지하였고, 미백 시간이 지날수록 증가하였다. 반면

Non-RF 군의 $h°$는 미백 후 감소하였고, 색 영역은 주황에서 붉은색으로 이동하였다. 미백 전 붉은 BF가 관찰되지 않는 Sound와 Non-RF 군을 BF 변수가 구분하는 능력을 receiver operating characteristic (ROC) 분석을 통해 확인하였다. ROC 분석 결과, 미백 후 ΔR과 $h°$ 변수의 민감도, 특이도, ROC 곡선 아래 영역(AUROC) 모두 향상된 것을 확인하였다. 특히 미백 5분 뒤 ΔR 변수의 민감도는 0.79에서 0.90으로 상당히 증가하였고, $h°$ 변수 역시 AUROC가 0.69에서 0.93으로 급격한 향상을 보였다. 미백 후 BF 변수 모두 0.83 이상의 높은 타당도로 우식성 변색을 구분할 수 있었다.

결론적으로 변색된 소와 열구에 BF-bleaching을 적용하면 BF의 색이 변화하며, 이를 통해 유기 착색이 미백으로 인해 제거되는 것을 확인하였다. 반면 우식성 변색은 미백 후 붉은 색조 영역이 유지되었다. 붉은 BF 강도와 BF 색조 각은 특히 미백 처치 5분 뒤 우식성 변색의 구분 능력이 향상되었다. BF 변수 모두 미백 후 높은 타당도로 우식성 변색을 구분하였다. 따라서 BF-bleaching은 임상에서 우식성 변색을 객관적으로 구분하고 우식 병소를 추적 관찰하는데 유망한 방법으로 활용 가능할 것이다.

핵심되는 말: 변색 우식 병소, 변색 소와 열구, 우식성 변색, 유기 착색, 생체형광, 치아 미백, 생체형광-미백 방법.